Energy Conversion and Management 353 (2026) 121216

Contents lists available at ScienceDirect

Energy Conversion and Management

journal homepage: www.elsevier.com/locate/enconman

# Comparative techno-economic analysis of a directly coupled production of methanol and formalin as example for improved hydrogen management in the chemical industry

Pia Münzer, Bruno Lacerda de Oliveira Campos, Ulrich Arnold *, Jörg Sauer

*Karlsruhe Institute of Technology, Institute of Catalysis Research and Technology, Hermann-von-Helmholtz-Platz 1, 76344 Eggenstein-Leopoldshafen, Germany*

ARTICLE INFO

*Keywords:*
Methanol
Formaldehyde
$H_2$ management
$CO_2$ utilization
Waste utilization
Techno-economic assessment
Process simulation

ABSTRACT

In the context of carbon–neutral production, sustainable $H_2$ will become a crucial resource and key element for the transformation of the chemical industry. In this study, the potential of inter-plant $H_2$ networks is demonstrated in the context of methanol and its derivatives. In order to assess the impact of the exploitation of untapped $H_2$-rich waste streams, a process chain for the directly coupled production of $CO_2$-based methanol and formaldehyde was chosen. It is shown that including a $H_2$ loop between a modified silver catalyst processes for formaldehyde production and the feed stream of $CO_2$-based methanol synthesis results in an increase in process performance as well as economic benefits. Directly coupled production leads to utilization ratios of 98% and 99% for $CO_2$ and $H_2$, respectively, while exergy efficiencies are improved by up to 4.5%pt. Economic evaluation shows that improved $H_2$ management not only yields savings in operational expenditures but also lowers capital investments. Over a wide range of assumed $H_2$ prices, small decentralized plants become more competitive when both subprocesses are directly linked. Minimum selling prices between 836 €·t$^{-1}$ and 852 €·t$^{-1}$ are reached for methanol in integrated plants, corresponding to a decrease of 3 to 13.5%pt when compared to separately operated $CO_2$-based methanol synthesis followed by conventional formaldehyde production.

## 1. Introduction

Transitioning to a carbon–neutral chemical industry will require the utilization of carbon dioxide ($CO_2$) as alternative carbon source in combination with sustainable hydrogen ($H_2$) for many industrial processes that are currently based on fossil resources. Examples of essential commodities that will be affected by this change in raw materials are ammonia, methanol ($CH_3OH$), and ethylene. Consequentially, in order to substitute conventional syngas feedstock a drastic increase in the demand for renewable $H_2$ is generally anticipated [1]. In 2024, global $H_2$ consumption was nearly 100 Mt, half of which was required for the production of ammonia and methanol [2]. Prompted by the increasing interest to use $H_2$ for power generation, energy storage and fuel synthesis, the demand is predicted to reach over 500 Mt by 2050 [1]. This poses an immense challenge for the chemical industry as not only green $H_2$ generation technologies have to be developed but also production capacities must be multiplied at the same time. In addition, sustainable $H_2$ production poses an economic strain that must be overcome. Even with the predicted decline in manufacturing costs by 2030, $H_2$ generation will be substantially more expensive during the transition period than it is today [1–4]. A way to minimize required $H_2$ amounts is the improvement of processes and process chains in terms of their $H_2$ efficiency. Numerous industrially relevant processes discharge $H_2$ as part of their flue gas. Well-known examples include ethylene and propylene production [5,6], chlor-alkali electrolysis [7–9], and formaldehyde ($CH_2O$) synthesis [10–12]. The refinement of $H_2$-rich waste streams could be a key lever to drive the transformation of chemical processes. Industrially significant process chains that include $H_2$-consuming and $H_2$-releasing steps are of special interest in this regard. A relevant example for such a pair is the production of methanol from syngas and the subsequent synthesis of formaldehyde. In the effort to attain carbon-neutrality, the initial carbon source is supposed to be shifted from fossil materials to sustainable sources such as $CO_2$. Recently, a lot of effort has been put into the development of $CO_2$-based methanol synthesis [13–21], which is now on the verge of commercialization [22,23]. Today's annual demand for methanol amounts to over 170 Mt [24]. For the production from $CO_2$, approximately 30 Mt of $H_2$ would stoichiometrically be necessary. Ideally, the used $H_2$ source is renewable or at least carbon–neutral, which leads to increased feedstock

* Corresponding author.
*E-mail address:* ulrich.arnold@kit.edu (U. Arnold).

https://doi.org/10.1016/j.enconman.2026.121216
Received 31 July 2025; Received in revised form 2 October 2025; Accepted 8 February 2026
Available online 14 February 2026

**Nomenclature**

*Acronyms*

| | |
|---|---|
| CEPCI | Chemical Engineering Plant Cost Index |
| COG | Coke oven gas |
| CZA | Supported copper-zinc-oxide |
| EIP | Eco-industrial parks |
| SCP | Silver catalyst process |

*Symbols*

| | |
|---|---|
| $a, b$ | Cost constants |
| $ACC$ | Annual capital costs |
| $C$ | Costs |
| $e$ | Specific exergy |
| $\dot{E}$ | Exergy flow |
| $EC$ | Equipment costs |
| $EX$ | Expenditures |
| $FCI$ | Fixed capital costs |
| $\dot{m}$ | Mass flow rate |
| $MSP$ | Minimum selling price |
| $n$ | Apparatus specific exponent |
| $N$ | Number, count |
| $NPC$ | Net production costs |
| $OL$ | Operating labor |
| $OPEX$ | Operational expenditures |
| $p$ | pressure |
| $P$ | Power |
| $\dot{Q}$ | Heat flow |
| $S$ | Size |
| $TCI$ | Total capital costs |
| $W$ | Wage |
| $WC$ | Working capital |
| $\eta$ | Efficiency, utilization ratio |

*Indices*

| | |
|---|---|
| $C$ | Consumables |
| $CO_2$ | Carbon dioxide |
| $D\&D$ | Development and distribution |
| $E$ | Exergy |
| $el$ | electric |
| $Feed$ | Feed stream |
| $H_2$ | Hydrogen |
| $in$ | input |
| $L$ | Lang factor |
| $O$ | Operator |
| $out$ | output |
| $Prod$ | Product stream |
| $PU$ | Process units |
| $R$ | Raw material |
| $ref$ | reference |
| $S$ | Shift |
| $U$ | Utilities |

costs in comparison to conventional value chains. At a price of 2.86 €·t$^{-1}$ for regenerative $H_2$ [1,3,4], an increase of 30.67 M€·a$^{-1}$ is to be expected. Approximately 30% of methanol produced is used for formaldehyde synthesis [25,26], for which formally one $H_2$ molecule must be released from the alcohol for each molecule of aldehyde formed. Depending on the implemented process, $H_2$ is either converted into water within the reaction system or it is combusted as part of waste gas valorization. In both cases, the $H_2$ potential of the value chain is not ideally utilized. Exploiting such untapped potential is especially vital in view of the rising demand for $H_2$ in connection with the effort to defossilize the chemical industry. In an attempt to evaluate the establishment of $H_2$ networks between otherwise independent processes, the production of $CO_2$-based methanol and subsequent formaldehyde synthesis serve as model value chain for the conducted techno-economic study. Both chemicals are vital $C_1$ building blocks of today's chemical industry so that their economic production is indispensable.

### 1.1. $H_2$ potential of industrial waste streams

In 2024, industrial waste streams were estimated to provide more than 14.5 Mt of available $H_2$ and thus to cover approximately 15% of global demand [2]. This number essentially includes $H_2$-rich byproducts from the petrochemical industry and refineries. Even though they are not directly part of the chemical industry, refineries deliver important feedstock for many chemical processes and therefore should be considered when discussing optimizing $H_2$ utilization. Among others, naphtha serves as initial material for olefin production. The relevance of olefins as chemical intermediates is emphasized by the anticipated ethylene capacity of 283 Mt in 2024 [27]. Each metric ton of ethylene is accompanied by circa 0.03 t of $H_2$, amounting to 8.5 Mt·a$^{-1}$ in total [5]. Not included in the aforementioned numbers are roughly 3 Mt of $H_2$ released as side product of 106 Mt of chlorine produced in 2024 [7,28]. Even though this $H_2$ stream is of high purity (99.9%), in Europe only about 48.5% of it are utilized chemically as for example in the synthesis of ammonia or hydrochloric acid [9]. Slightly more than 38% were used for steam and heat generation, leaving 13.5% of $H_2$ from the chlor-alkali industry completely untapped.

In addition to the mentioned chemical uses, about 30 Mt of $H_2$ contained in residues from industrial units like coke ovens and steam crackers were predicted to be used for internal heat or electricity generation in 2024 and thus not effectively utilized as chemical raw material [2]. Coke oven gas (COG) contains between 39% and 65% of $H_2$ making it especially interesting for investigations on $H_2$ recovery [29–31]. The gaseous product from coke ovens offers roughly 15 Mt of $H_2$ each year. In China, COG is already applied as raw material for a small number of methanol plants as a way of efficient $H_2$ separation [29]. In the majority of steel works, however, the $H_2$-rich stream is still used as fuel in coke oven batteries.

With 23 Mt·a$^{-1}$ to 27 Mt·a$^{-1}$ of formaldehyde produced via partial oxidation of methanol over silver catalysts, at least 0.5 Mt·a$^{-1}$ of $H_2$ are released during reaction [10,12,24–26,32]. Because no additional thermal energy is needed for internal purposes, the $H_2$-rich off-gas from installed absorbers is combusted in order to supply process steam to adjacent processes [10–12]. The remainder of the worldwide demand for formaldehyde of over 40 Mt is gained from methanol oxidation over iron-molybdenum-vanadium oxides [10,12]. In this case, no $H_2$ is contained in the product stream and thus no $H_2$ side product can be tapped into neither for chemical nor thermal use. If global formaldehyde production was to be carried out in silver catalyst processes (SCP) only, as of today over 1 Mt of $H_2$ could potentially be utilized.

Another example of $H_2$ formed as byproduct is given by the synthesis of hydrocyanic acid. Both of the industrially most relevant processes still offer the possibility to increase $H_2$ efficiency. While in the Andrussow process the released $H_2$ is contained in the reaction mixture and utilized to provide the needed energy inside the reaction chamber, the reaction and combustion are spatially separated in the competing BMA process (German abbreviation *hydrocyanic acid from methane and ammonia*) [33–36]. With over 70 vol% of $H_2$, the product gas from the latter process is especially interesting for $H_2$ recovery [33,34].

In summary, it can be noted that there is still a significant $H_2$

potential in the chemical industry that is not exploited efficiently. Closing this gap by making unused $H_2$ quantities of waste streams accessible could facilitate the transformation of the chemical industry towards carbon-neutrality.

### 1.2. Process coupling and optimization of $H_2$ efficiency

Facing the anticipated increase in $H_2$ demand, short-term solutions are needed in order to kickstart a prompt rollout of the targeted carbon–neutral economy [37]. Hence, maximizing internal $H_2$ use of industrial processes [38] and optimizing the utilization of $H_2$-rich byproducts [39] have been suggested to boost carbon-neutrality quickly. While the importance of $H_2$-rich waste streams and the need to expand the exploitation of this resource are recognized [39–42], only a limited number of studies have been published regarding the recovery of $H_2$ from byproducts of the chemical industry. In contrast, $H_2$ networks are already implemented in refineries and are still being optimized further [43–48]. More general work on inter-plant integration via the exchange of $H_2$ streams between refineries and petrochemical plants has also been published [49–52].

The retrieval of $H_2$ from byproduct gases in the iron and steel industry has also been discussed extensively in literature and is already practiced in some industrial sites [53–72]. Published studies either address the separation and purification of $H_2$ or the utilization of accumulating $H_2$-rich streams for the generation of syngas or base chemicals. Considered integrated syntheses are dominated by methanol production [61–70] but also include ammonia synthesis [68,69], dimethyl ether production [71], and methanation [72]. In general, the studies conclude that the exploitation of gaseous waste streams from steel works leads to an increased energy or exergy efficiency as well as economic benefits.

The concept of eco-industrial parks (EIP) was introduced 35 years ago in an effort to minimize waste, unused byproducts and energy losses of manufacturing processes [73–77]. Worldwide, known implemented projects often include networks for (waste) water, steam, heat and to some extent also the exchange of material waste streams that can be harnessed chemically by neighboring plants or companies [78–81]. So far, only few concrete examples have specifically evaluated $H_2$ networks or loops in the chemical industry [82,83]. Thun and Chew conceptualized an EIP connecting a cement plant and steel mill with a total of eight chemical units relevant for carbon-neutrality like methanol and Fischer-Tropsch synthesis, methanation and biodiesel production [84]. Kuznetsov et al. integrated co-electrolysis and Fischer-Tropsch synthesis by recycling water and $H_2$ as well as light fuel gases between the units in order to reduce overall emissions of the combined production of syngas and synthetic fuel [85]. In addition to $CO_2$ emissions, the need for fuel and utilities could also be lowered by the implemented exchange of resources.

Of all chemical systems, dehydrogenation reactions are a reasonable target for a first attempt on improving the related $H_2$ efficiency. Published works have focused on propylene and acetaldehyde production in this context [86,87]. Methanol and its derivatives also merit a closer look given their relevance for many value chains and the increased demand for $H_2$ of a targeted $CO_2$-based synthesis. A large number of techno economic assessments of the $CO_2$-based methanol synthesis has been published [88–102]. Most studies validate, that the intended consumption of sustainable $H_2$ is the primary cause of the significantly higher production costs when compared to the established fossil-based process. In order to reduce the overall amount of purchased raw material, Charoensuppanimit et al. integrated a small-scale $CO_2$-based methanol plant to the production site of sodium methoxide by exploiting the $H_2$ byproduct released during the process [103]. The gained methanol was then in turn used for sodium methoxide synthesis. At the considered production capacities, financial savings resulting from the utilization of the $H_2$-rich side product were counterbalanced by increased investment costs to build the additional methanol unit on site. It was indicated that the suggested process would be profitable if the market price of methanol increased in the future or plant size was considerably increased.

Roughly 30% of methanol are employed in order to produce formaldehyde as intermediate for the production of different chemicals [25,26]. The formally required elimination of $H_2$ from the molecule during synthesis gives cause to study the opportunity to exchange $H_2$-rich streams between methanol and formaldehyde plants. Mantei et al. investigated the possibility to integrate the $H_2$ side product of anhydrous formaldehyde production (Technology Readiness Level 3) to the preceding methanol synthesis as part of large-scaled production of oxymethylene dimethyl ethers from $CO_2$ and renewable $H_2$ [104]. The authors showed, that total energy utilization of the production was enhanced by recycling the $H_2$-rich stream. However, an increased formation of CO as product from formaldehyde decomposition due to high reaction temperatures required larger purge fractions. Together with higher investment costs caused by the rougher operating conditions of anhydrous formaldehyde synthesis and additionally required purification of $H_2$, this fact led to the nullification of any economic benefits caused by an increase in $H_2$ efficiency.

Until now, no studies have been published considering the oxidative dehydrogenation of methanol over silver catalysts in the context of $H_2$ exchange networks. Anhydrous formaldehyde synthesis, as considered by Mantei et al. [104], will not be commercially available in the near future and hence does not offer a short-term solution for $H_2$ shortage in the transition period. In contrast, the oxidative dehydrogenation, as regarded in the presented work, has been successfully implemented in the industry for over 100 years [10,11]. Large scale SCP production sites offer ample opportunity for substantial $H_2$ savings and thus should be considered when discussing $H_2$ efficiency in the methanol value chain. While the concept of Charoensuppanimit et al. [103] was designed for large scale sodium methoxide production, the integrated methanol plant with a capacity of approximately 7 $kt \cdot a^{-1}$ did not allow for the exploitation of benefits offered by commercial production sites following the economy of scale. A combined operation of $CO_2$-based methanol synthesis and the SCP presents a unique opportunity to rapidly enhance $H_2$ efficiency of one of the most relevant base chemicals in the chemical industry.

Previously published work indicates that the overall $H_2$ potential is exploited more effectively and $CO_2$ utilization ratios could be increased, when a modified SCP for formaldehyde synthesis is integrated in a $CO_2$-based methanol production site [105]. The identified positive effects of a $H_2$ loop included between both processes are an incentive for a more detailed evaluation of the suggested concept.

### 1.3. Scope of study

As example for the potential of $H_2$ networks in the chemical industry, different options for the realization of $CO_2$-based process chains for the production of methanol and formaldehyde are evaluated regarding their performance as well as rentability. Directly coupled plant operation, as proposed in previous work [105], is compared to independently operated production sites. Methanol can be viewed as intermediate for formaldehyde production from $CO_2$ and $H_2$ in all cases but is additionally produced as final product in some scenarios. System boundaries include the conditioning of the gaseous raw materials, methanol synthesis, downstream processing of raw methanol and the following preparation for and execution of formaldehyde production via a modified SCP. External inputs encompass $H_2$, $CO_2$ or $N_2$, $O_2$, water, air and electricity while outputs comprise methanol, aqueous formaldehyde solutions, water, combustion exhaust gases and electricity.

Important operating parameters are determined and a techno-economic evaluation is performed to identify relevant economic factors and their influence on production costs. Goal of the presented cost calculations is an assessment of the effect $H_2$ recirculation might have on process performance and economics. With a typical uncertainty of

±30% [106], estimated prices of products are not to be interpreted as exact numbers but rather serve as comparative values. For easier evaluation, the costs are nevertheless compared with the current market prices of fossil product equivalents.

## 2. Process description

As one of the fundamental building blocks of the chemical industry, methanol is produced on a large scale in centralized plants. It is then distributed to other production sites to serve as raw material as exemplary shown for subsequent formalin production in Fig. 1. Due to the necessity of an intermediate transportation step, the conventional supply chain offers only limited potential for inter-plant integration and the associated improved utilization of input materials.

In the following, a description of the $CO_2$-based synthesis of methanol and consecutive production of formaldehyde performed in a SCP is given. Afterwards, a directly coupled process chain with integrated $H_2$ loop is introduced.

### 2.1. $CO_2$-based methanol synthesis

Methanol is typically produced via the hydrogenation of carbon oxides (Eq. (1) and Eq. (2)) [13,25,107]. The desired synthesis reactions are accompanied by the reverse water–gas shift and water–gas shift reaction (Eq. (3)). Process conditions of industrial plants are optimized for the conversion of CO over supported copper-zinc-oxide (CZA) catalysts [13,25,107,108]. In the context of carbon–neutral methanol production, the substitution of fossil carbon sources like syngas by $CO_2$ is subject of recent and ongoing research [13–21]. A $CO_2$-rich feedstock inevitably leads to more water in the product, causing an increased effort for the purification of methanol. Additionally, new catalysts have to be developed, that are more resistant against deactivation by water [109,110].

$$CO + 2H_2 \rightleftharpoons CH_3OH \quad (1)$$

$$CO_2 + 3H_2 \rightleftharpoons CH_3OH + H_2O \quad (2)$$

$$CO_2 + H_2 \rightleftharpoons CO + H_2O \quad (3)$$

The economic sourcing of large quantities of $CO_2$, e.g. from the atmosphere or from industrial waste streams, and of green $H_2$ is seen as key factor in the successful implementation of $CO_2$-based methanol production on industrial scale [88–98]. Stoichiometrically, three mol of $H_2$ are necessary to convert one mol of $CO_2$ (see Eq. (2)), leading to an increased $H_2$ demand of $CO_2$-based methanol production when compared to the fossil route.

### 2.2. Formaldehyde synthesis

Formaldehyde is the raw material for the production of a variety of resins [111], plastics [112], and other valuable chemicals [113–115]. Industrially, formaldehyde is mainly produced via the oxidative partial dehydrogenation of methanol (Eq. (4) and Eq. (5)) over polycrystalline silver particles [10,12]. As the catalyst requires $O_2$ to convert methanol, unwanted combustion reactions of formaldehyde (Eq. (6)) and $H_2$ (Eq. (7)) have to be considered as well. Due to high reaction temperatures, the thermal decomposition of the aldehyde (Eq. (8)) into $H_2$ and CO is also relevant to the reaction system. If the SCP includes water as diluent in the feed stream, it is referred to as water ballast or BASF process [11,12]. In this case, in addition to the aqueous formaldehyde a $H_2$-rich waste gas is collected from the concluding absorption column of the plant. Since the main component of the gas stream is $N_2$, a separation and further utilization of the contained $H_2$ is not profitable [116–118]. Instead, the off-gas is often used for steam generation as a way of waste heat recovery [10–12].

$$CH_3OH + 0.5\,O_2 \rightarrow CH_2O + H_2O \quad (4)$$

$$CH_3OH \rightleftharpoons CH_2O + H_2 \quad (5)$$

$$CH_2O + O_2 \rightarrow CO_2 + H_2O \quad (6)$$

$$H_2 + 0.5\,O_2 \rightarrow H_2O \quad (7)$$

$$CH_2O \rightleftharpoons CO + H_2 \quad (8)$$

### 2.3. Directly coupled production with $H_2$ loop

Fig. 2 displays a detailed flowsheet of the suggested process chain with integrated $H_2$ loop. In a first step, methanol is gained in a $CO_2$-based synthesis before the raw alcohol is passed on to the SCP or sent to a distillation column for further purification. Both processes are linked by the recirculation of the $H_2$-rich gas released at the head of the absorption column (A).

At the beginning of the process chain, both $CO_2$ and $H_2$ are compressed ($C^1$ to $C^4$) and preheated ($H^1$ to $H^3$) before they enter the reactors. Three consecutive CZA-filled isothermal multi tubular modules ($R^1$ to $R^3$) with intermediate product condensation are considered as suggested by Campos et al. [88]. Reaction temperatures of each module are regulated by boiling water cooling [25,107]. Steam leaving the cooling system is overheated by purge stream combustion (C) and utilized for electricity generation in a turbine (T). After the product gas leaves the final conversion unit, unreacted feed gases are separated from the produced raw methanol in a flash (F) and fed back to the initial compression stage ($C^1$). The liquid product is sent to the inlet of the subsequent SCP. If the capacity of methanol production exceeds the amount required for formaldehyde synthesis, the remaining raw

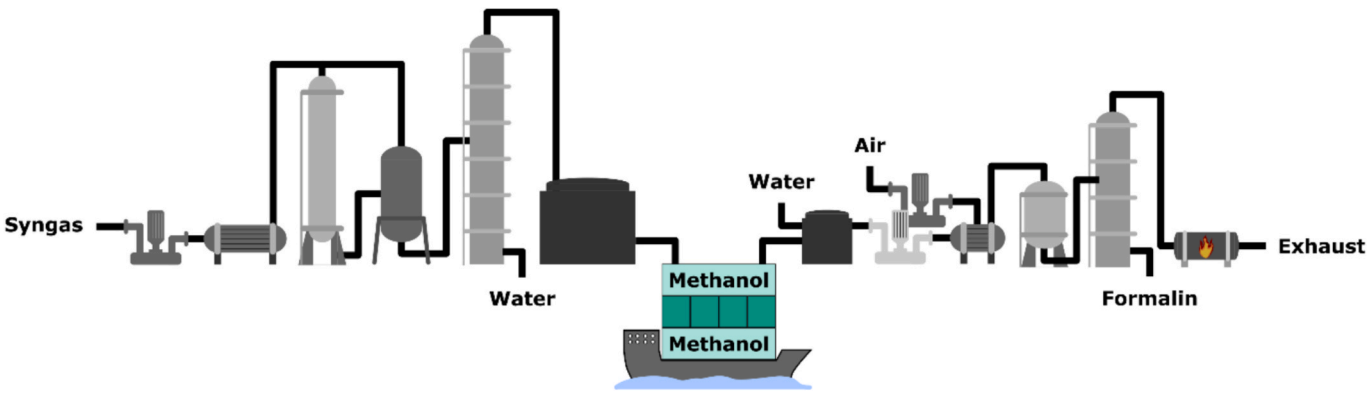


**Fig. 1.** Schematic flow diagram of the conventional process chain for the production of methanol and formaldehyde including intermediate transport.

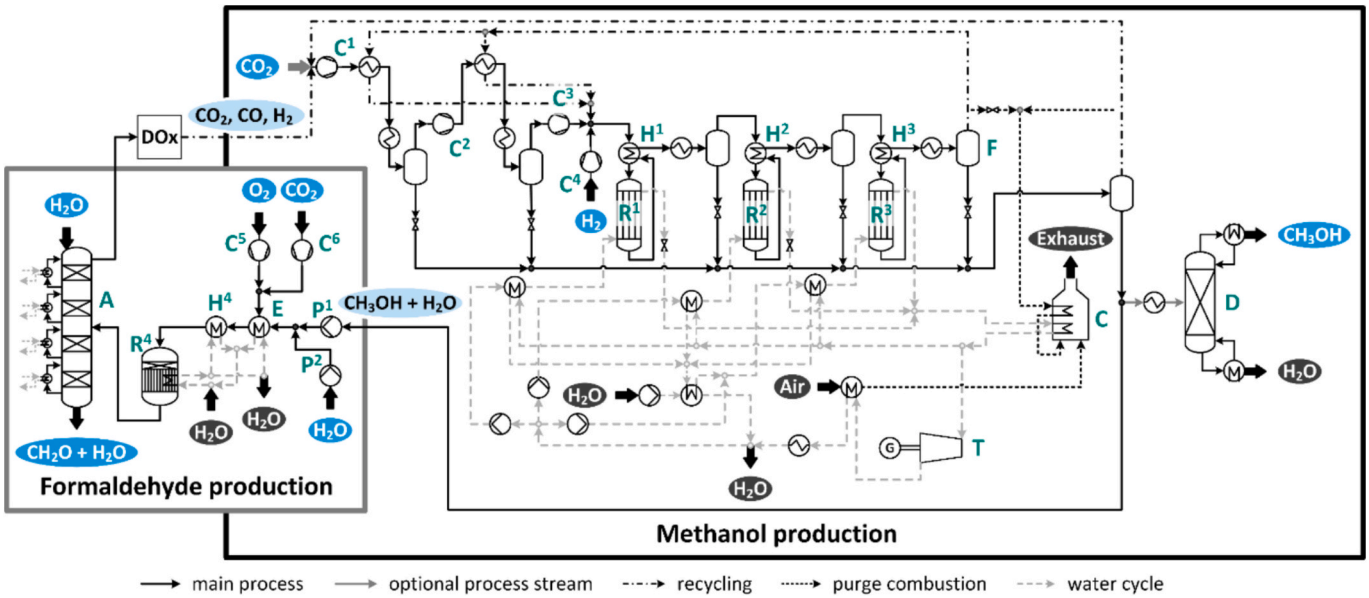


**Fig. 2.** Process flow sheet for the directly coupled production of methanol and formaldehyde based on $CO_2$ and $H_2$.

methanol can be led to a distillation column (D) to reach the wanted purity for further applications.

The water-methanol mixture leaving the reactor cascade ($R^1$ to $R^3$) is directly introduced to the inlet of a modified SCP. After the water-to-methanol ratio is adjusted in the inlet stream ($P^1$ and $P^2$), the liquids are evaporated (E). While in a conventional set up air is added during evaporation, a mixture of $O_2$ and $CO_2$ is supplied instead in the suggested coupled process design ($C^5$ and $C^6$). The feed stream is overheated ($H^4$) and converted over polycrystalline silver particles in a fixed bed reactor ($R^4$). To minimize thermal decomposition of formaldehyde, gas-hourly space velocities of $10^5$ to $2.5{\cdot}10^5$ $h^{-1}$ are implemented and a swift quenching of the product gas is ensured within 0.2 s after leaving the catalyst bed [12,119]. The recovered waste heat is used to provide energy for evaporation (E) and overheating ($H^4$). As a concluding step, formaldehyde is chemically absorbed in water (A) to stabilize the product. The aldehyde reacts not only with water to form methylene glycols ($MG_n$, $HO(CH_2O)_nH$, Eq. (9)) but also with unreacted methanol to produce hemiformals ($HF_n$, $CH_3O(CH_2O)_nH$, Eq. (10)) [10,120,121].

$$CH_2O + H_2O \rightleftharpoons MG_1 \tag{9.1}$$

$$MG_1 + (n-1)\,CH_2O \rightleftharpoons MG_n \tag{9.2}$$

$$CH_2O + CH_3OH \rightleftharpoons HF_1 \tag{10.1}$$

$$HF_1 + (n-1)\,CH_2O \rightleftharpoons HF_n \tag{10.2}$$

Typically, the aqueous solution, called formalin, contains 37–55 wt% of the aldehyde. The overhead product of the absorption column (A) consists of the released $H_2$ as well as $CO_2$, CO and traces of unconverted $O_2$. After deoxygenation [122] the stream is recycled to the initial compression of methanol production and hence both processes are directly connected. Additional $H_2$ is added ($C^4$) to reach the desired $H_2$-to-$CO_2$ ratio for methanol synthesis. If needed, fresh $CO_2$ is also introduced ($C^1$–$C^3$) to enable larger methanol capacities.

## 3. Methods

As basis for process evaluation and techno-economic assessment, flowsheet simulations were performed with the help of Aspen Plus. Feedstock and exergy utilization as well as operational expenditures and investment costs were determined to analyze overall performance of the process chain.

### 3.1. Process simulation

All regarded processes were implemented as flowsheet simulations in Aspen Plus V11. For most equipment the Non-Random Two-Liquid property method with a second set of binary parameters (NRTL2) was chosen. In accordance with literature, the multi tubular reactor modules for methanol synthesis were implemented using the Redlich-Kwong-Soave equation of state including Huron-Vidal mixing rules (RKSMHV2) [123–125]. To describe the reaction system of methanol synthesis (Eq. (1) to Eq. (3)), a kinetic model, proposed by Campos et al. [126], was integrated as Langmuir-Hinshelwood-Hougen-Watson (LHHW) model. Further details can be found in the Supporting Information. Rigorous plug flow reactors (RPlug) with co-current flow of boiling cooling water were used as representation for each of the modules. Because the reaction mechanism of formaldehyde synthesis over silver catalysts is still not fully determined [127–131], the fixed bed reactor was integrated as stoichiometric converter module (RStoic). Data on methanol conversion and product yield as well as the composition of the process off-gas were taken from literature to determine the extent of the regarded reactions (Eq. (4)–(8)) [10–12,119,132–134]. The procedure for calculating product composition is described in the Supporting Information. In order to ensure a realistic portrayal of the chemisorption of formaldehyde, a model developed by Bongartz et al. was incorporated to the simulations [135]. It includes ideal gas properties (IDEAL) as well as nonideal liquids (UNIFAC). Present permanent gases, such as $CO_2$, CO, $H_2$ and $O_2$, were considered to be soluble in the liquid phase. A rigorous fractionation unit (RadFrac) was applied to simulate a four-stage column. Heat released during the reactive absorption was removed on the highest and lowest level with the gas stream entering on the bottom and water being supplied to the top of the tower. All heat exchangers were implemented as counter-current shell-and-tube configuration (HeatX), if they were utilized for heat integration. If the units were not part of the steam cycle, basic heater blocks (Heater) with integrated cooling water utility were used. A minimal temperature approach of 10 °C was assumed for all heat exchangers. Pressure changers (Compr) were adapted including a polytropic ASME method with an efficiency of 72%.

All simulations were run using the Broyden method with a tolerance of $10^{-4}$ to reach convergence. An error of $10^{-6}$ was allowed for all process units. A detailed list of all process units and the chosen operating parameters can be found in Section C of the Supporting Information.

Most relevant simulation results are also given in the supplementary material.

#### 3.1.1. Methanol

For all simulations $H_2$ and $CO_2$ were added in a ratio of 3:1 and assumed to be obtained with a purity of 100% from cleaned industrial waste streams and electrolysis, respectively. In order to limit the required feed excess and the associated costs, a purge fraction of 1% was selected in agreement with other comparable studies [123,136]. Each of the three consecutive reactor modules had a length of 10 m with varying numbers of parallel tubes between 1195 and 5085 to adjust to the different production capacities. Reaction conditions were set at 259 °C and 70 bar. To optimize heat transfer, the pressure of the boiling water cooling was adapted individually for each reactor module, leading to pressure levels of 41.5 bar to 43 bar. The water streams were entered to the cooling system at the according boiling temperature and an average heat transfer coefficient of 285 $W{\cdot}m^{-2}{\cdot}K^{-1}$ was assumed for all reactor modules [88]. To further utilize the produced steam, it is overheated with the exhaust from purge gas combustion and sent to a turbine for electricity generation. Purge streams are burned with an air-to-fuel ratio of 1.1 [137]. A minimum molar purity of 99% was chosen for the distilled methanol product. Different scales ranging from 110 $kt{\cdot}a^{-1}$ to 500 $kt{\cdot}a^{-1}$ were considered for preceding methanol production.

#### 3.1.2. Formaldehyde

Referring to industrial capacity, an annual formaldehyde production of 90 kt was assumed [10]. Methanol and water were added in a weight ratio of 1.5, while 0.4 mol of $O_2$ per mol of methanol were introduced to the system [10,12,127]. In a conventional SCP, this results in a molar feed composition of approximately 25% methanol, 10% $O_2$, 30% water and 35% of $N_2$. For the adapted SCP feed, $O_2$ was assumed to be produced as side product from electrolysis installed for $H_2$ generation. $CO_2$ replaced $N_2$ as diluent in a ratio of 0.95 in relation to the specific heat capacity of both substances to ensure heat management of the exothermic reaction system. The educt is then composed of 28 mol% methanol, 11 mol% $O_2$, 34 mol% water, and 27 mol% $CO_2$. With stronger explosion-inhibiting abilities of $CO_2$ in comparison to $N_2$, the slight shift in composition should not affect process safety as the operating point is also outside of explosion limits of methanol-air-water mixtures [138–142]. Reaction parameters were set at 680 °C and 1.2 bar and are within the range of typical values for SCP in water-ballast configuration [10,11]. During the simulations it was assumed that the introduction of large amounts of $CO_2$ does not interfere with the reaction system of formaldehyde formation (Eq. (4)–(8)). The effect any impurities contained in the feed streams may have on the catalyst were not considered explicitly but rather assumed to be included in the values of industrial conversion and yields as well as kinetic models taken from literature. This matter was not factored in for the $CO_2$-modified SCP either, because impurities common for $CO_2$ streams like $H_2S$, $SO_2$, CO, $H_2O$, $H_2$, $NO_x$, $N_2$ and $O_2$ are either part of the reaction network or also present in the conventional feed stream using air [143,144]. Adjusting composition to meet the required specifications of the $CO_2$ stream is considered to be part of the capture process and therefore is not included in the suggested process scheme. The gaseous product stream is absorbed in water, resulting in an aqueous formaldehyde solution of 37 wt% also known as formalin [10–12]. A four-stage column was selected for the separation task.

### 3.2. Evaluation of process performance

For the comparison of process performance three characteristic variables were considered. To evaluate the potential benefits regarding $H_2$ utilization, overall hydrogen efficiency $\eta_{H_2}$ was calculated from mass balances as shown below:

$$\eta_{H_2} = \frac{\dot{m}_{H_2,in} - \dot{m}_{H_2,out}}{\dot{m}_{H_2,in}} \tag{11}$$

Here, $\dot{m}_{H_2,in}$ is the mass stream of hydrogen entering the feed stream of methanol production at the beginning of the process chain. The hydrogen amount contained in purge streams is summarized as $\dot{m}_{H_2,out}$.

In addition, an assessment of total $CO_2$ conversion was carried out by estimating the according utilization ratio $\eta_{CO_2}$ from fed $CO_2$ amounts ($\dot{m}_{CO_2,in}$) and cumulated discharged quantities ($\dot{m}_{CO_2,out}$):

$$\eta_{CO_2} = \frac{\dot{m}_{CO_2,in} - \dot{m}_{CO_2,out}}{\dot{m}_{CO_2,in}} \tag{12}$$

Overall energy use was evaluated by determination of exergy efficiency $\eta_{Ex}$ of the sub-processes as well as the total process assembly following Eq. (13). It is calculated by relating the exergy of products $E_{Prod}$ to the sum of exergy from feed streams $E_{Feed}$, electrical power $P_{el}$, and heat $\dot{Q}$ introduced to the process.

$$\eta_E = \frac{\dot{E}_{Prod}}{\dot{E}_{Feed} + P_{el} + \dot{Q}} = \frac{\sum \dot{m}_{Prod,i} \bullet e_{Prod,i}}{\sum \dot{m}_{Feed,i} \bullet e_{Feed,i} + P_{el} + \dot{Q}} \tag{13}$$

The exergy flow $\dot{E}_i$ of a material stream is defined as product of its mass flow $\dot{m}_i$ and specific exergy $e_i$. In the case of multiple relevant streams their exergy values are added to obtain the total exergy flow.

### 3.3. Economic assessment

A techno-economic assessment was performed following a standardized procedure as is common practice in literature [106,145]. Main result of the considered analysis is the minimum selling price (*MSP*, Eq. (14)) which includes net production costs (*NPC*, Eq. (15)) and expenditures for distribution as well as product and process development ($EX_{D\&D}$) related to the amount $\dot{m}_i$ of intermediate and final products of the process chain. For the calculation of the *MSP* a production site in Europe was assumed. A regional factor of 1.1 [106] was included in the estimation of equipment costs. The *MSP* does not include profit margins and is thus lower than the actual market price.

$$MSP\left[\frac{€}{t}\right] = \frac{NPC + EX_{D\&D}}{\dot{m}_i} \tag{14}$$

$$NPC\left[\frac{€}{t}\right] = \frac{ACC + OPEX}{\dot{m}_i} \tag{15}$$

Production costs are dependent on the annual capital costs (*ACC*, Eq. (16)) as well as operational expenditures (*OPEX*, Eq. (21) and Eq. (22)) and are related to the product capacity $\dot{m}_{Prod}$. The *ACC* annualize the fixed capital investment (*FCI*, Eq. (17)) and working capital (*WC*) while taking an interest rate (*IR*) and plant lifetime (*PL*) into account [106,145].

$$ACC = \frac{(1+IR)^{PL} \bullet FCI \bullet IR}{(1+IR)^{PL} - 1} + IR \bullet WC \tag{16}$$

$$FCI = F_L \bullet \sum EC_i = 0.9 \bullet TCI \tag{17}$$

$$TCI = FCI + WC \tag{18}$$

In order to determine the *FCI*, the costs of process equipment (*EC*) have to be calculated and are multiplied with an installation factor $F_L$, also known as Lang factor, of 4.86 [146]. This can either be done based on reference costs $EC_{ref}$ of previously built plants (Eq. (19)) or on cost curves (Eq. (20)) given in literature [90,106,145]. In both cases, the size *S* of the designed process and an apparatus specific exponent *n* are used to adjust equipment cost. Plant scale is either related to a reference capacity $S_{ref}$ or used in connection with cost constants *a* and *b*. Price inflation was corrected to 2023 with the Chemical Engineering Plant

Cost Indices (*CEPCI*) of the current and reference year. Ultimately, total capital investment (*TCI*, Eq. (18)) includes both *FCI* and *WC*.

$$EC = EC_{ref} \bullet \left(\frac{S}{S_{ref}}\right)^{n} \bullet \frac{CEPCI_{2023}}{CEPCI_{ref}} \tag{19}$$

$$EC = a + b \bullet S^{n} \bullet \frac{CEPCI_{2023}}{CEPCI_{ref}} \tag{20}$$

Expenses for plant operation are typically divided into direct ($OPEX_{dir}$, Eq. (21)) and indirect operating expenditures ($OPEX_{ind}$, Eq. (22)). The former are linked to raw materials ($C_R$), utilities ($C_U$) and other consumables ($C_C$) that are needed for the production of the desired product. Indirect costs must be covered regardless of whether the plant is running or not and include operating labor (*OL*), supervision, maintenance, taxes and plant overhead among others. The elements mentioned later are expressed as a function of *FCI* or *OL*, respectively [106,145].

$$OPEX_{dir} = \sum C_R + \sum C_U + \sum C_C \tag{21}$$

$$OPEX_{ind} = 1.04 \bullet OL + 0.08 \bullet FCI \tag{22}$$

Costs for operating labor (Eq. (23)) are made up of the count of shifts ($N_S$) needed for continuous plant operation of 8000 h·a$^{-1}$ as well as the number of operators ($N_O$, Eq. (24)) per shift and an average wage ($W_O$). The number of operators can be estimated in relation to the quantity of main process units ($N_{PU}$) [147].

$$OL = N_S \bullet N_O \bullet W_O \tag{23}$$

$$N_O = (6.29 + 0.23 \bullet N_{PU})^{0.5} \tag{24}$$

Considered feedstock, material and labor costs for the estimation of operating expenditures are summarized in Table 1.

## 4. Results

Different scenarios were implemented in Aspen Plus to evaluate the potential of the proposed concept. All cases were designed for a constant annual formaldehyde capacity to guarantee comparability. The suggested modified SCP was combined with methanol plants of different scales. In addition to the directly coupled process chain, separate production of $CO_2$-based methanol followed by classic formaldehyde production was regarded. Cases were named after their methanol production capacity in kt•a$^{-1}$ (110, 200, 500) and their mode of operation (separate (s) or coupled (c)). Fossil methanol synthesis followed by an independently operated conventional SCP served as reference for the presented study.

### 4.1. Process performance

In order to evaluate process performance, mass balances were primarily taken in to account. Needed values were taken from the performed flowsheet simulations and served as basis for the calculation of $H_2$ efficiencies and $CO_2$ utilization ratios. Exergy balances were drawn up and regarded as measure of energy efficiency.

#### 4.1.1. Mass balances

Table 2 lists educt and product mass flows for the considered simulations. Formaldehyde production was fixed at 90 kt·a$^{-1}$ in all scenarios and a concentration of 37.04 ± 0.02 wt% was achieved for the liquid stream leaving the absorption column. The amount of methanol produced varied only little, when comparing the simulation results for separate sub-processes (110s, 200s, and 500s) to the corresponding coupled process chain (110c, 200c, and 500c). With a maximum deviation of 0.2%, very good comparability is given and the effect of process coupling can be evaluated based on the values taken from Aspen Plus. Distilled methanol products reached purities of 99.08 ± 0.08 mol% while intermediate methanol products designated for formaldehyde production contained 62.41 ± 0.29 wt% of the alcohol. It also becomes evident, that not only is the needed amount of fresh $H_2$ reduced, but also $CO_2$ discharge is lowered by directly linking methanol and formaldehyde production. Recycling the released $H_2$ from the SCP, lowered the demand of fresh $H_2$ by 0.29 t·h$^{-1}$. At the same time $CO_2$ release was decreased by 1.74 t·h$^{-1}$ to 2.02 t·h$^{-1}$ which equals an annual reduction in $CO_2$ emissions of 13.9 kt·a$^{-1}$ to 16.1 kt·a$^{-1}$ that can be directly correlated to the coupling of both process steps. In total, the proposed concept utilizes 1.30 ± 0.05 t of $CO_2$ per ton of methanol resulting in an annual consumption of 136.5 kt·a$^{-1}$ (110s) to 676.3 kt·a$^{-1}$ (500c).

#### 4.1.2. $H_2$ efficiency and $CO_2$ utilization ratio

After implementing and optimizing the different scenarios, simulation results were used to evaluate process performance (Table 3). For the calculation of $\eta_{H_2}$ and $\eta_{CO_2}$ (see Eq. (11) and Eq. (12)) needed mass streams were taken from Aspen Plus. As expected, both utilization ratios increase from 86.7% to 95.2% and 89.6% to 95.7% with increasing scale of methanol synthesis, if the production facilities were considered separately. At smaller production capacities the quantity of $H_2$ discharged in the off-gas of the SCP corresponds to a larger proportion of the total amount supplied to the process chain, leading to lower utilization ratios. Similarly, $CO_2$ contained in flue gases and purge streams from both production sites, equal a bigger fraction of the volume introduced to methanol synthesis. With rising methanol capacities, the rejected streams become relatively small when compared to the according feed streams and thus material efficiencies are higher. When both processes are directly connected by recycling the released $H_2$, $\eta_{H_2}$ and $\eta_{CO_2}$ are nearly constant for all considered cases, taking on averaged values of 98%. Relative increase of both values is largest for the smallest considered scale (110s vs. 110c) with an increase of 10.8%pt for $\eta_{H_2}$ and 9.0%pt for $\eta_{CO_2}$. For a production site with a methanol capacity of 500 kt·a$^{-1}$, linking both subprocesses leads to an improvement of 2.4%pt regarding $H_2$ input and 2.2%pt in terms of $CO_2$ discharge. Therefore, by enhancing the utilization of $H_2$, economies of scale are offset in the regarded range of capacity and thus smaller decentralized plants are favorable. Minor deviations can be attributed to slight variations in the

**Table 1**
Assumed feedstock, material and labor costs for the estimation of operational expenditures.

| Item | Unit | Costs | Reference |
|---|---|---|---|
| $H_2$ | €·t$^{-1}$ | 2857 | [1,3,4] |
| $CO_2$ | €·t$^{-1}$ | 38 | [148–152] |
| $CO_2$ certificates (2025) | €·t$^{-1}$ | 55 | [153] |
| Fossil Methanol | €·t$^{-1}$ | 539 | [154] |
| Electricity | €·MWh$^{-1}$ | 105 | [145] |
| Cooling water | €·t$^{-1}$ | 0,00125 | [145] |
| Clean water | €·t$^{-1}$ | 2 | [145] |
| CZA catalyst | €·kg$^{-1}$ | 20.39 | [155,156] |
| Silver catalyst | €·kg$^{-1}$ | 444.50 | [157] |
| Operator wage | €·a$^{-1}$ | 50,000 | [158] |

**Table 2**
Resulting educt and product mass flows taken from Aspen Plus for the considered $CO_2$-based process chains with methanol and formaldehyde production separately operated (s) and directly coupled (c) at different methanol capacities (110 kt·a$^{-1}$, 200 kt·a$^{-1}$, 500 kt·a$^{-1}$).

| Parameter | 110s | 200s | 500s | 110c | 200c | 500c |
|---|---|---|---|---|---|---|
| $\dot{m}_{H_{2,in}}$ [t·h$^{-1}$] | 2.62 | 4.78 | 12.13 | 2.33 | 4.49 | 11.84 |
| $\dot{m}_{H_{2,out}}$ [t·h$^{-1}$] | 0.35 | 0.40 | 0.58 | 0.06 | 0.11 | 0.29 |
| $\dot{m}_{CO_{2,in}}$ [t·h$^{-1}$] | 19.04 | 34.82 | 88.25 | 17.42 | 32.98 | 86.34 |
| $\dot{m}_{CO_{2,out}}$ [t·h$^{-1}$] | 1.98 | 2.43 | 3.82 | 0.24 | 0.50 | 1.80 |
| $\dot{m}_{CH_3OH}$ [kt·a$^{-1}$] | 108.24 | 197.52 | 499.76 | 108.32 | 197.84 | 499.68 |
| $\dot{m}_{CH_2O}$ [kt·a$^{-1}$] | 90.08 | 90.08 | 90.08 | 90.08 | 90.08 | 90.08 |

**Table 3**
Calculated process performance indicators $\eta_{H_2}$ and $\eta_{CO_2}$ for the considered $CO_2$-based process chains with methanol and formaldehyde production separately operated (s) and directly coupled (c) at different methanol capacities (110 kt·a$^{-1}$, 200 kt·a$^{-1}$, 500 kt·a$^{-1}$).

| Parameter | 110s | 200s | 500s | 110c | 200c | 500c |
|---|---|---|---|---|---|---|
| $\eta_{H_2}$ [%] | 86.7 | 91.6 | 95.2 | 97.5 | 97.6 | 97.6 |
| $\eta_{CO_2}$ [%] | 89.6 | 93.0 | 95.7 | 98.6 | 98.5 | 97.9 |

composition of the material flows for the different simulations and to rounding errors.

#### 4.1.3. Exergy efficiency

Exergy efficiencies $\eta_{Ex,i}$ were calculated for both the separate production stages individually as well as for the complete process chain and are listed in Table 4. Nearly constant numbers for $\eta_{E,CH_3OH}$ validate comparability of the differently scaled simulations in Aspen Plus. Slight deviations of less than 0.3%pt can again be led back to rounding errors and minimal differences in stream compositions. The resulting values of individually operated methanol plants between 78.1% and 78.4% are in good agreement with studies published prior to this work [88,159,160]. Since the same simulation flowsheet was considered for formaldehyde synthesis, $\eta_{E,CH_2O}$ equals 72.1% in all three cases of separate operation. Overall energy utilization $\eta_{E,total}$ increases from 56.4% to 73.4% with growing scale of methanol production as proportionally more methanol is available for direct marketing. The higher efficiency of the subprocess then consequently also leads to an overall improvement in exergy efficiency.

Fig. 3 exemplary shows the distribution of exergy flows for separately operated methanol and formaldehyde production at capacities of 110 kt·a$^{-1}$ and 90 kt·a$^{-1}$, respectively. Regarding the exergy provided, approximately 97.5% are supplied in the form of $H_2$ with the rest being electrical power and water. The Sankey diagram also illustrates that the main causes for exergy destruction are the reactor modules, heat exchangers as well as the absorption column needed to stabilize the gained formaldehyde.

While the same factors play a role for the directly coupled scenarios (Fig. 4), the need for fresh $H_2$ is reduced due to the implemented recycle. This leads to an improvement of $\eta_{Ex,CH_3OH}$ in all scenarios resulting in values as high as 88.4% in the smallest methanol plant. Since the absolute volume of recirculated $H_2$ stays constant throughout the simulations, the improvement is more significant for smaller methanol productions. Exergy efficiencies of the according formaldehyde section remain almost identical for all cases, again indicating good comparability of the simulations. With around 69%, $\eta_{E,CH_2O}$ is reduced when compared to independent operation of the plants. This decrease stems from the loss of the steam byproduct produced in the conventional process chain as way of waste utilization (Fig. 3). However, this deficit is compensated by the increase in $\eta_{E,CH_3OH}$, leading to an improvement of overall exergy efficiency with $\eta_{E,total}$ reaching values between 60.9% and 74.6%. At lower production capacities $\eta_{E,total}$ can be increased by 4.5%pt by directly coupling both production steps. Although the effect is less significant at larger scales, energy use could still be improved by 1.2%pt nonetheless. As the smallest scenario produces the exact amount of methanol needed for formaldehyde production, it shows the maximum potential of the suggested process coupling.

**Table 4**
Exergy streams and efficiencies calculated for the considered $CO_2$-based process chains with methanol and formaldehyde production separately operated (s) and directly coupled (c) at different methanol capacities (110 kt·a$^{-1}$, 200 kt·a$^{-1}$, 500 kt·a$^{-1}$).

| Parameter | 110s | 200s | 500s | 110c | 200c | 500c |
|---|---|---|---|---|---|---|
| $\dot{E}_{in}$ [MW] | 108.68 | 198.83 | 503.70 | 96.47 | 187.28 | 491.75 |
| $\dot{E}_{CH_3OH,out}$ [MW] | 0 | 70.53 | 308.42 | 0 | 70.85 | 308.23 |
| $\dot{E}_{CH_3OH,CH_2O}$ [MW] | 85.18 | 84.88 | 84.88 | 85.22 | 84.88 | 85.02 |
| $\dot{E}_{CH_2O}$ [MW] | 58.81 | 58.81 | 58.81 | 58.84 | 58.78 | 58.79 |
| $\dot{E}_{steam}$ [MW] | 2.58 | 2.58 | 2.58 | 37.63 | 57.65 | 124.73 |
| $\dot{E}_{des}$ [MW] | 46.87 | 66.91 | 133.89 | 11.80 | 11.85 | 11.86 |
| $\eta_{E,CH_3OH}$ [%] | 78.4 | 78.2 | 78.1 | 88.3 | 83.2 | 80.0 |
| $\eta_{E,CH_2O}$ [%] | 72.1 | 72.1 | 72.1 | 68.9 | 69.1 | 69.0 |
| $\eta_{E,total}$ [%] | 56.4 | 66.3 | 73.4 | 60.9 | 69.2 | 74.6 |

### 4.2. Economic assessment

After it became evident that process performance is enhanced for directly linked production sites, the effect of process coupling on economic viability was also assessed. Simulation results were used as basis for the calculation of operational expenditures as well as the dimensioning of the implemented process units in order to estimate investment costs. A detailed list of resulting expenses and additional diagrams regarding the economic assessment for both processes in the considered scenarios are given in the Supporting Information.

#### 4.2.1. Capital investment

Fig. 5 a)–d) illustrate the distribution of annual capital costs per ton of methanol. For the purpose of clarity, only methanol plants with capacities of 110 t·a$^{-1}$ and 500 t·a$^{-1}$ are shown. When considering separately operated sites (Fig. 5 a) and b)), main contributions to investment costs could be allocated to the compressors, feed pre-heaters and distillation columns. As the costs of heat exchangers were appraised by modularization, whenever the calculated area exceeded the allowed range of the according cost function, their absolute value may be overestimated. It is the cause for the shift in significance of feed pre-heaters from small (110s) to large (500s) plants while all other components lose importance. However, since the same procedure was applied to all cases, a comparison of the scenarios is still valid. Investment costs per ton of methanol are lowered from 187 €·t$^{-1}$ to 133 €·t$^{-1}$ with increasing production capacity.

Directly coupled operation leads to a decrease in *ACC* of methanol production, because the distillation column can either be omitted, if all of the produced methanol is supplied to the SCP (case 110c), or can at least be downsized, if only a part of the alcohol is directly utilized further (cases 200c and 500c). Changes to the column inevitably lead to a shift in distribution of capital investment. Fig. 5 c) and d) illustrate that especially for small coupled process chains (110c) the influence of feed compression and feed pre-heating on overall costs are increased while the distillation becomes less substantial. At a production capacity of 110 kt·a$^{-1}$, investments can be reduced to 155 €·t$^{-1}$ by implementing the suggested $H_2$ loop. Because the distillation is only reduced in size but cannot be left out completely, savings are less significant for large plants (500c) resulting in annual costs of 127 €·t$^{-1}$.

In case of a separately operated SCP (Fig. 5 e)) the evaporator, absorption column and furnace needed for off-gas combustion hold the largest shares of investment costs. Per ton of formaldehyde produced 38 €·t$^{-1}$ can be attributed to capital investment. By introducing the $H_2$-rich waste gas into the feed of a linked methanol plant, a furnace is no longer needed and thus the influence of the absorber and evaporator on *ACC* are increased. This elimination causes the annual investment to drop to 27 €·t$^{-1}$. Because the implemented SCP remains unchanged regardless of the capacity of methanol production, only two plant configurations need to be considered.

In summary, it can be concluded that by establishing the suggested $H_2$ loop investment costs can be reduced for both plants due to elimination or downsizing of the distillation column and waste stream combustion.

#### 4.2.2. Operational expenditures

Although the mode of plant operation has an influence on the ab-

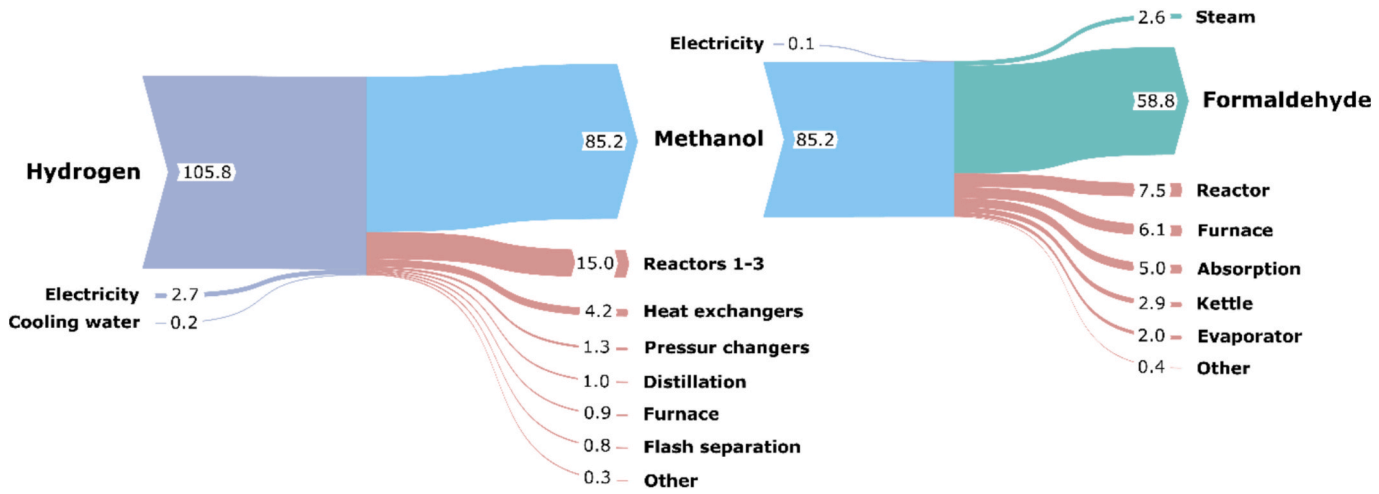


**Fig. 3.** Distribution of exergy flows (given in MW) for separately operated methanol and formaldehyde production at capacities of 110 kt·a$^{-1}$ and 90 kt·a$^{-1}$ (case 110s), respectively.

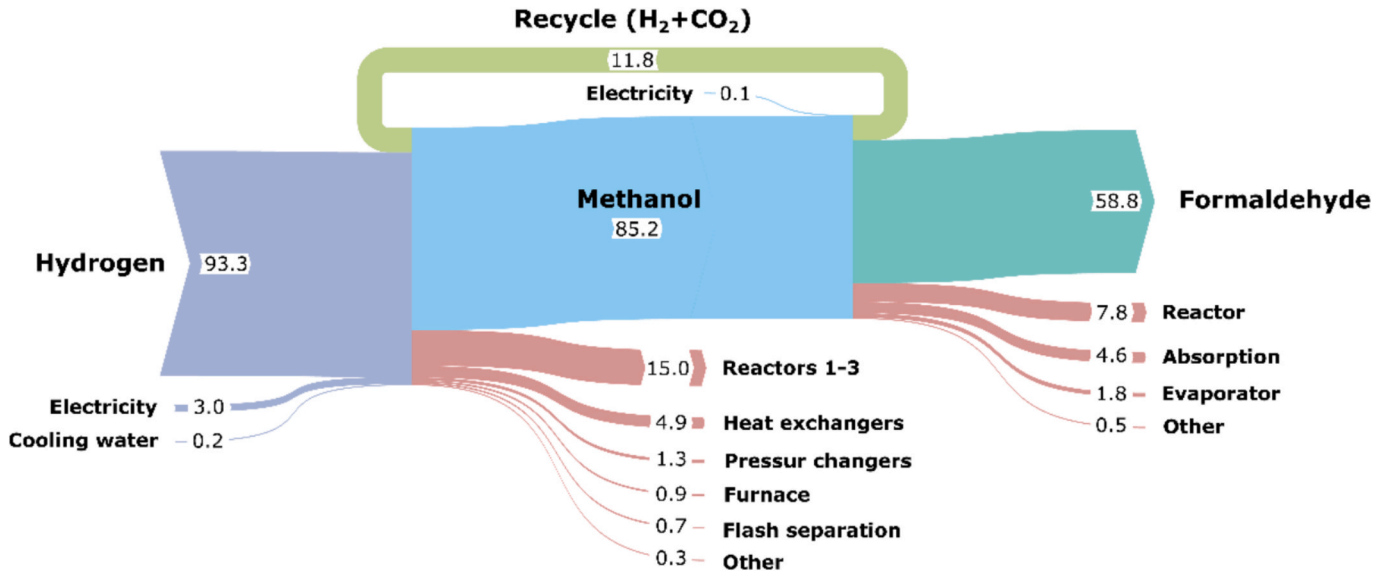


**Fig. 4.** Distribution of exergy flows (given in MW) for directly coupled methanol and formaldehyde production at capacities of 110 kt·a$^{-1}$ and 90 kt·a$^{-1}$ (case 110c), respectively.

solute value of *OPEX*, it has only little impact on cost distribution for the considered process chain. In order to illustrate the effect of plant scale, Fig. 6 a) and b) exemplary show the *OPEX* of $CO_2$-based methanol production with integrated $H_2$ loop for capacities of 110 kt·a$^{-1}$ and 500 kt·a$^{-1}$. For all considered cases, the largest share can be attributed to the required sustainable $H_2$, matching the results from other techno-economic studies [88–102]. While $H_2$ is responsible for 76% of OPEX in the largest configuration (500c), its proportion is reduced to approximately 71% for small plants (110c). This shift in allocation is due to an increase in indirect *OPEX* which are directly proportional to higher levelized *ACC* of small sites. No substantial change in importance of $CO_2$ and electricity for overall operational expenses can be attributed to plant size. Labor costs become less significant for large systems, because the number of process units remains constant regardless of plant scale (see Eq. (24)) while the amount of product is increased. For a separately operated process chain, *OPEX* decrease from 779 €·t$^{-1}$ to 732 €·t$^{-1}$ when production capacity is increased from 110 kt·a$^{-1}$ to 500 kt·a$^{-1}$, respectively. For the designed process with included $H_2$ loop, operational expenditures vary from 695 €·t$^{-1}$ (110c) to 714 €·t$^{-1}$ (500c). Reduced spending for smaller coupled plants can be led back to the increased $H_2$ efficiency and the resulting lowered purchasing costs for this limiting resource.

Regarding the SCP, the mode of operation again correlates to the absolute value of *OPEX* but does not change the contributions of the required resources. Because the plant scale remains unchanged throughout the different cases, no assessment of the role of plant size can be made in the context of operational costs. For this reason, only one representative pie chart is given for the production of formaldehyde. With a share of about 96%, operational costs of the SCP (Fig. 6 c)) are essentially determined by the spending for methanol. In contrast, influence of indirect OPEX and labor costs can be neglected. Total expenditures for independent plants range from 1080 €·t$^{-1}$ (500s) to 1214 €·t$^{-1}$ (110s). With *OPEX* of formaldehyde production depending on both *ACC* and operational expenses of methanol synthesis, final values of coupled production are not linearly correlated to methanol capacity. Instead, savings in *ACC* are offset by higher *OPEX* with increased plant size. Thus, SCPs coupled with medium sized methanol synthesis (200c) have larger expenses than small (110c) and large (500c) sites. Operational costs per ton of formaldehyde range from 979 €·t$^{-1}$ (500c) to 1003 €·t$^{-1}$ (200c). A list of OPEX for both processes is given in the

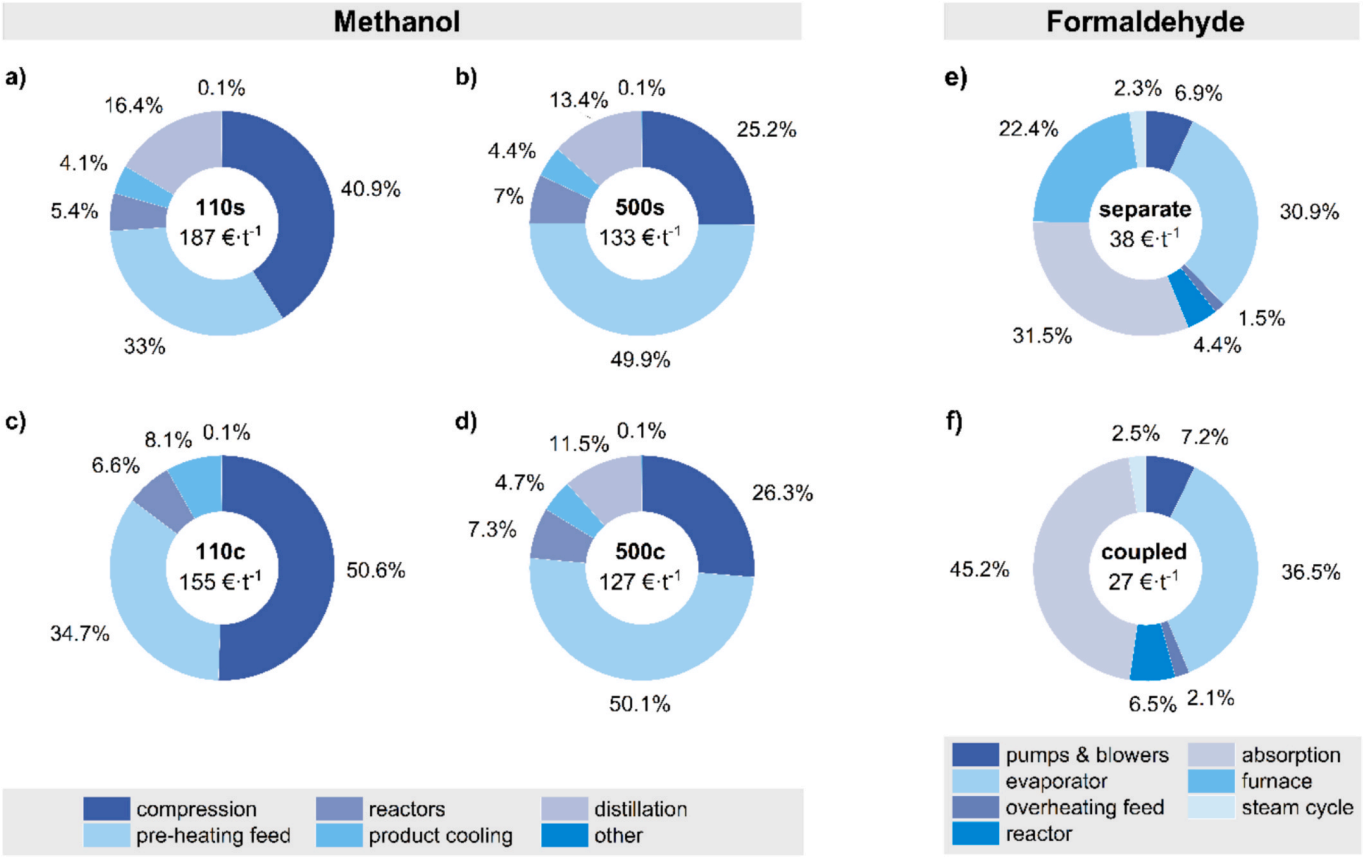


**Fig. 5.** Distribution of annual capital costs. a)-d) *ACC* (€·t$^{-1}$ of methanol) for plants with methanol capacities of 110 kt·a$^{-1}$ and 500 kt·a$^{-1}$, e) + f) *ACC* (€·t$^{-1}$ of formaldehyde) for SCP in separate (s) and coupled (c) operation. The name of the scenario and the respective absolute values are given in the center of the doughnut plots. The shares of contributing components are provided outside the circle.

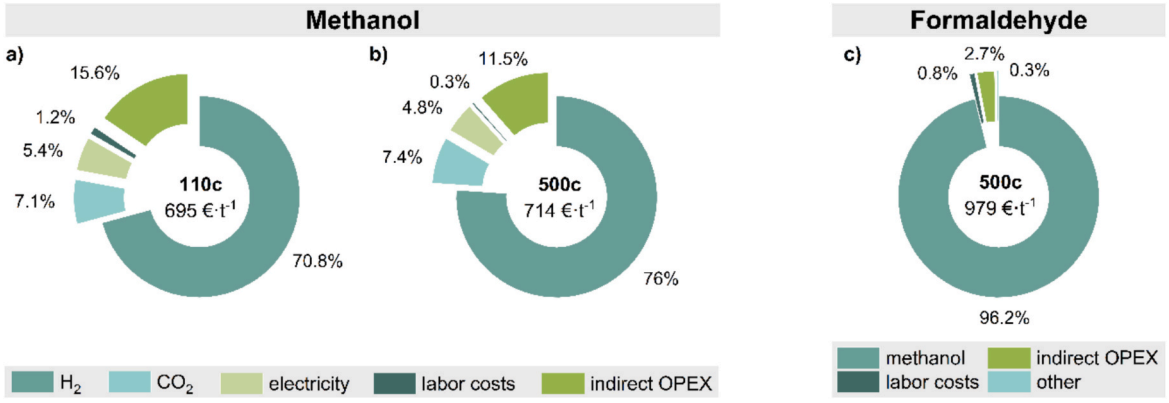


**Fig. 6.** Distribution of operational expenditures (*OPEX*) exemplary shown for coupled (c) process chains with production capacities of 110 kt·a$^{-1}$ and 500 kt·a$^{-1}$. a) + b) *OPEX* (€·t$^{-1}$ of methanol) for plants with methanol capacities of 110 kt·a$^{-1}$ and 500 kt·a$^{-1}$, c) *OPEX* (€·t$^{-1}$ of formaldehyde) for SCP in coupled (c) operation. The name of the scenario and respective absolute values are given in the center of the doughnut plots. The shares of contributing components are provided outside the circle.

Supporting Information for all considered scenarios.

#### 4.2.3. *Minimum selling price of methanol*

Fig. 7 illustrates the minimum selling price per ton of methanol produced. In order to determine the *MSP*, the total production capacity was used, including both the methanol sold as end product as well as the amount intended as raw material for formaldehyde production. Following the economy of scale, the costs per ton of product are reduced with increasing production capacity, when comparing the scenarios regarding the separate operation of the processes. Prices range from 861 €·t$^{-1}$ (500s) to 973 €·t$^{-1}$ (110s) and are listed in Table 5. More than half of the costs (52.0% to 58.3%) can be attributed to the sustainable $H_2$ consumed. The second largest share is related to the investment costs (*ACC*) and makes up 13.9% to 17.6% of expenditures. As expected, annual capital costs lose importance with increasing scale of the production site. Fig. 7 also indicates that, while most of the described dependencies also apply to the directly coupled process chains, there are some changes concerning cost distribution as well as overall costs. Most

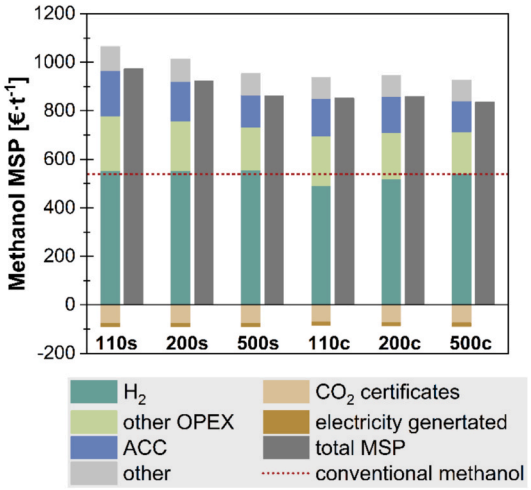


**Fig. 7.** Calculated minimum selling price (*MSP*) per ton of methanol for separately operated (s) and directly coupled (c) processes at different scales (110 kt·a$^{-1}$, 200 kt·a$^{-1}$ and 500 kt·a$^{-1}$). The market price of conventional methanol (539 €·t$^{-1}$ in 2024) is given as reference [154].

**Table 5**
Calculated minimum selling prices (*MSP*) of methanol and formaldehyde for separately operated (s) and directly coupled (c) processes at different methanol capacities (110 kt·a$^{-1}$, 200 kt·a$^{-1}$ and 500 kt·a$^{-1}$).

| Product | *MSP* [€·t$^{-1}$] | | | | | |
|---|---|---|---|---|---|---|
| | 110s | 200s | 500s | 110c | 200c | 500c |
| Methanol | 973 | 922 | 861 | 852 | 858 | 836 |
| Formaldehyde | 1384 | 1316 | 1236 | 1123 | 1131 | 1105 |

importantly, the expenditures for the utilized $H_2$ is reduced for all cases in which the absorption off-gas is recycled. As already indicated during performance evaluation, the effect is strongest for small plants and lessens with growing capacity. Ultimately, the recirculation of $H_2$ reduces *MSP* by 13 €·t$^{-1}$ (500c) to 62 €·t$^{-1}$ (110c).

With the mentioned savings, small production sites become financially more viable than medium-scale plants and thus represent a good alternative to large systems within the evaluated range. After the subtraction of 70 €·t$^{-1}$ for abated $CO_2$ emissions, overall selling costs are 837 €·t$^{-1}$, 851 €·t$^{-1}$ and 858 €·t$^{-1}$ for the cases 500c, 110c and 200c, respectively. Compared to the corresponding separately operated plants, a cost reduction of 2.9% to 12.4% could be achieved by directly coupling both process steps.

All directly coupled scenarios are cheaper than any of the separately operated plants regardless of their size. Even at the smallest capacity, coupled production is more cost efficient than large scale production sites in independent operation.

In the considered scenarios, the applied $CO_2$ as well as electricity, mainly employed for the operation of the compressors, have little influence on the final methanol price. The same is true for the costs incurred for product distribution and research. Saved certificates for avoided $CO_2$ emissions are considered to be sold and thus subtracted from the final costs as well as the electricity generated in the turbine of the steam cycle.

Compared to the assumed price of 539 €·t$^{-1}$ of fossil methanol, the estimated methanol costs may initially appear relatively high. However, it must be pointed out that cost calculations, as they are presented in this work, typically exhibit an accuracy of ±30%. Actual *MSP* of methanol from the presented process chain with integrated $H_2$ network, may consequently be as low as 585 €·t$^{-1}$ (500c) and thus considerably closer to the chosen reference value. It should also be considered that market prices of fossil methanol are subject to fluctuations and in Europe have been as high as 625 €·t$^{-1}$ to 700 €·t$^{-1}$ recently [161].

#### 4.2.4. Minimum selling price of formaldehyde

In good agreement with literature [12], formaldehyde production costs are primarily influenced by the price of methanol. In the presented study, it makes up 84% to 85% of the *MSP* of the aldehyde (Fig. 8). As a consequence, all described trends identified for the profitability of methanol production also apply to the price of formaldehyde. The associated costs for all scenarios are presented in Table 5 and range from 1105 €·t$^{-1}$ (500c) to 1384 €·t$^{-1}$ (110s). It is found, that for separately operated process chains, the production costs per ton of formaldehyde equal 1.43 times the *MSP* of methanol. For the coupled production this factor is reduced to 1.32. This can be ascribed to the absence of the furnace needed for off-gas combustion in the conventional SCP as well as the omission of expenditures for the purification and shipment of methanol. In comparison, calculated prices for fossil formaldehyde range from 810 €·t$^{-1}$ to 1020 €·t$^{-1}$ depending on the considered prices for fossil methanol between 540 €·t$^{-1}$ and 700 €·t$^{-1}$ [154,161]. For the production of formaldehyde in a $CO_2$-based process chain, an increase of costs of between 8.3% and 39.6% must be accepted for the suggested coupled production. Separate operation of both plants leads to escalations of 21.2% to 70.9%.

### 4.3. Sensitivity

Techno-economic analysis showed that production costs of $CO_2$-based methanol are dominated by the price of $H_2$ and indirect *OPEX*. It is therefore of interest to investigate their influence in further detail to make a statement on the feasibility of the suggested coupled process chain. With indirect *OPEX* being proportional to investment cost, it cannot be independently adjusted for a fixed plant setup as it is considered here. The conducted sensitivity study thus focuses on prices for $H_2$, $CO_2$ and electricity as well as resulting $CO_2$ abatement costs. Only methanol sales were considered for the sensitivity calculations presented in the following. Since formaldehyde prices predominantly depend on methanol purchase, all identified correlations for the *MSP* of methanol can be directly transferred to formaldehyde costs. Hence, a standalone sensitivity study for the SCP is not necessary.

Fig. 9 presents the *MSP* of methanol plotted against $H_2$ price for separate (Fig. 9 a) and coupled (Fig. 9 b) process chains. For all scenarios, methanol prices show a linear dependency on $H_2$ costs. It becomes evident that small-scaled plants with independent subprocesses

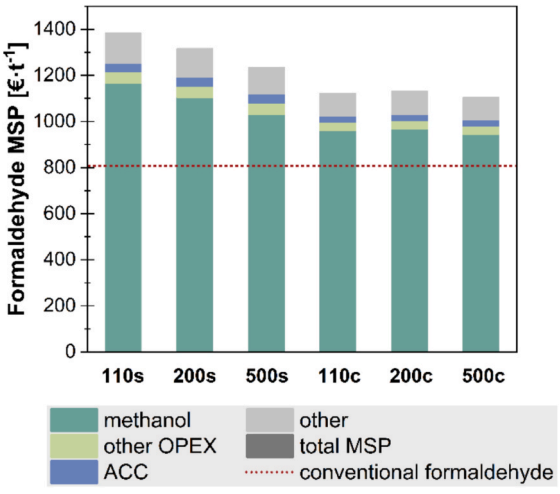


**Fig. 8.** Calculated minimum selling price (*MSP*) per ton of formaldehyde for separately operated (s) and directly coupled (c) processes at different methanol capacities (110 kt·a$^{-1}$, 200 kt·a$^{-1}$ and 500 kt·a$^{-1}$). The calculated price of conventional formaldehyde (810 €·t$^{-1}$ in 2024) is given as reference.

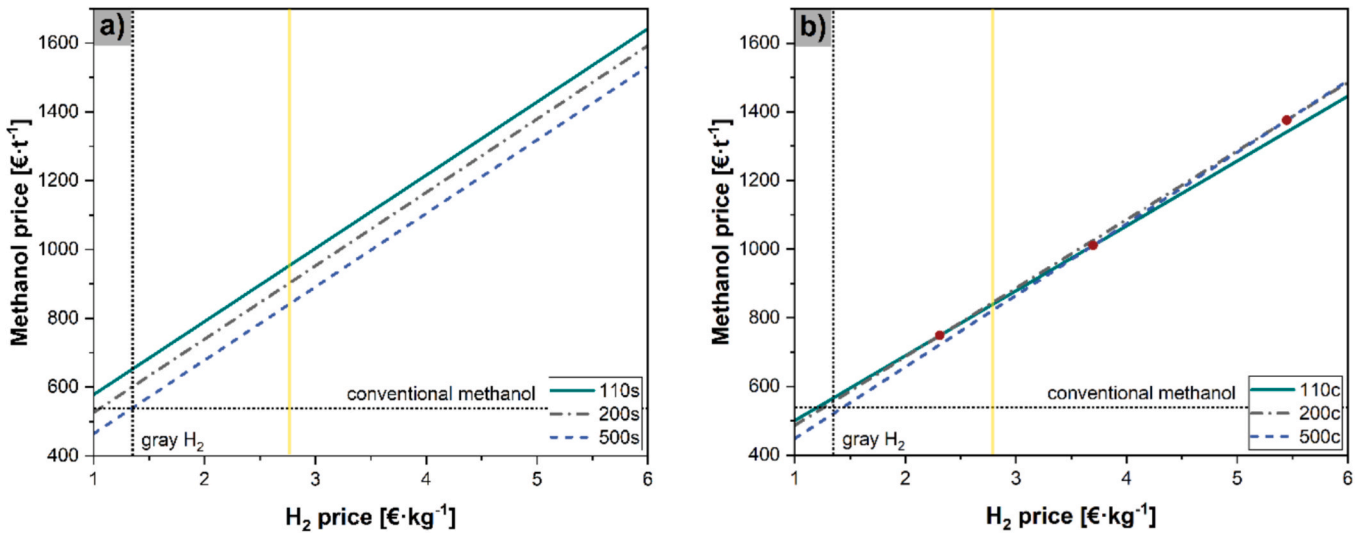


**Fig. 9.** *MSP* of methanol for separate (a)) and coupled (b)) process chains at different methanol capacities (110 kt·a$^{-1}$, 200 kt·a$^{-1}$ and 500 kt·a$^{-1}$) in dependence of $H_2$ price. The market price of conventional methanol (539 €·t$^{-1}$ in 2024) is given as reference [154]. Yellow lines mark initial values of the cost factor, red circles indicate a change in superiority of the regarded plant scales.

cannot compete with conventional methanol production even if green $H_2$ prices would drop to 1 €·kg$^{-1}$. In contrast, medium-sized and large plants fall below this threshold at values of 1.06 €·kg$^{-1}$ (200s) and 1.34 €·kg$^{-1}$ (500s). The latter breakeven point is nearly identical to the current market value of fossil $H_2$ of 1.35 €·kg$^{-1}$ [4].

When considering the sensitivity of directly coupled process chains towards $H_2$ costs, it becomes clear that at some point all cases can compete with fossil methanol. Intersections with the base cost curve can be found at values between 1.20 €·kg$^{-1}$ and 1.43 €·kg$^{-1}$ dependent on plant scale. Unlike for separately operated subprocesses, the cost curves are no longer parallel lines, but instead exhibit different slopes in relation to the extent of influence of $H_2$-recycling on costs. Due to the larger share of recycled $H_2$ relative to total demand, methanol prices of small coupled plants (110c) depend less strongly on $H_2$ market prices. They are thus more robust to fluctuating prices of renewable $H_2$ production. Where the lines cross (red circles in Fig. 9 b)), there is a change in superiority of the plant scales depicted. Small production sites will be more profitable than medium-scaled plants as long as $H_2$ prices are 2.33 €·kg$^{-1}$ and above. Small sites are also more beneficial than large ones, if $H_2$ costs amount to more than 3.70 €·kg$^{-1}$. Medium-sized processes are only favorable over large productions, if sustainable $H_2$ prices would increase to over 5.45 €·t$^{-1}$. With European market prices of fossil methanol currently between 625 and 700 €·t$^{-1}$ [161], $H_2$ production costs of up to 2.21 €·t$^{-1}$ would be compensated by the suggested directly coupled operation of methanol and formaldehyde plants.

Even though electricity prices do not seem to have a substantial impact on operational expenditures of methanol production, this cost factor should not be disregarded. Because approximately 60% of the price of electrochemically generated $H_2$ can be ascribed to required electricity [162–164], electricity prices also indirectly influence the selling price of $CO_2$-based methanol in this study. In order to evaluate the sensitivity towards electricity costs, prices were varied between 25 €·kWh$^{-1}$ and 200 €·kWh$^{-1}$. At low electricity prices, large scale $CO_2$-based methanol productions reach *MSP* that are comparable to conventional prices for both separate (500s, Fig. 10 a)) and integrated (500c, Fig. 10 b)) sites. Small plants including a $H_2$ network (110c) become less expensive than medium-sized (200c) and large (500c) sites at electricity prices of 65 €·kWh$^{-1}$ and 162 €·kWh$^{-1}$ (red circles in

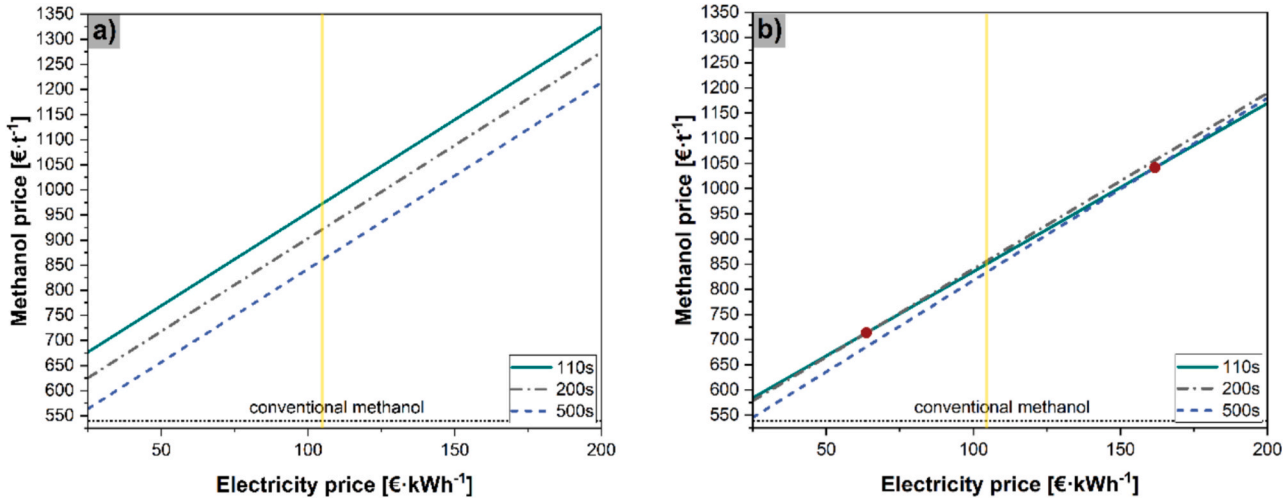


**Fig. 10.** *MSP* of methanol for separate (a)) and coupled (b)) process chains at different methanol capacities (110 kt·a$^{-1}$, 200 kt·a$^{-1}$ and 500 kt·a$^{-1}$) in dependence of electricity price, taking into account the impact on $H_2$ costs. The market price of conventional methanol (539 €·t$^{-1}$ in 2024) is given as reference [154]. Yellow lines mark initial values of the cost factor, red circles indicate a change in superiority of the regarded plant scales.

Fig. 10 b)), respectively.

To procure $CO_2$ as alternative carbon source, many different technologies like absorption, membranes and direct air capture may be considered [165–169]. Estimated capture costs vary strongly depending on the technology as well as made assumptions during calculations, giving cause to a wide range of possible $CO_2$ prices. The impact of $CO_2$ sourcing on methanol prices of the different case studies is shown in Fig. 11. Methanol prices display a linear dependency on $CO_2$ supply costs, yet even a reduction to 0 €·t$^{-1}$ does not lead to competitive market prices of $CO_2$-based methanol regardless of the mode of plant operation. For separately operated sites, economy of scale is effective at any assumed $CO_2$ price, making large plants most profitable (Fig. 11 a)). In contrast, small methanol plants with integrated $H_2$ loop (100c) become more profitable than large scaled systems (500c) at a $CO_2$ price of 191 €·t$^{-1}$, as is shown in Fig. 11 b) (red circle). Again, due to larger shares of recycled $CO_2$ that is formed during formaldehyde synthesis relative to total demand, small directly coupled plants are the least sensitive to changes in $CO_2$ prices. Thus, small sites offer most stable methanol prices for varying carbon capture costs. Of the coupled production sites, medium-sized systems (200c) lead to the highest methanol prices over the complete range of considered $CO_2$ capture costs.

In order to assess what abatement costs would be necessary to make $CO_2$-based methanol competitive with today's market, the value of $CO_2$ certificates was varied from 50 to 300 €·t$^{-1}$ [3]. Calculations were made for a constant $H_2$ price of 2.86 €·kg$^{-1}$. For independent methanol plants, only large installations could fall below the current market price of methanol, as is shown in Fig. 12 a). $CO_2$ abatement costs would have to reach 288 €·t$^{-1}$ in order to lower the *MSP* of $CO_2$-based methanol to the current market price. When considering coupled facilities (Fig. 12 b)), all plant scales reach the targeted value of 539 €·t$^{-1}$ within the range of sensitivity. $CO_2$ certificates have to reach 300 €·t$^{-1}$, 297 €·t$^{-1}$, and 273 €·t$^{-1}$ for the regarded production capacities in ascending order. At a value of 190 €·t$^{-1}$ (red circle in Fig. 12 b), $CO_2$ abatement costs outweigh the benefit of increased $H_2$ efficiency when comparing the cases 110c and 200c. At higher $CO_2$ prices, medium-sized methanol plants directly coupled to the SCP are more economic than small integrated production sites. With increased plant size the scale of installations outweighs the influence of $CO_2$-abatement costs.

Fig. 13 provides a summary of the change in *MSP* of methanol for all considered scenarios when the investigated parameters change by ±20%. The tornado plot clearly shows that $H_2$ (dark green) and electricity prices (light green) are crucial to methanol manufacturing costs and therefore should be defined as precisely as possible for a sound techno-economic assessment of $CO_2$-based methanol production. In comparison, the dependence of *MSP* on uncertainties in prices for $CO_2$ sourcing (greenish-blue) and sold certificates (yellow, plotted inversely) is relatively weak. This again highlights the urgency of optimizing $H_2$ efficiency of the methanol value chain, which is particularly true for small decentralized production sites. While the nominal *MSP* of small coupled plants (110c) is 852 €·t$^{-1}$, the same value will only be reached in separately operated sites (110s) if the implemented price of $H_2$ is reduced by 20%.

Finally, the effect elevated operating pressures of the SCP $p_{SCP}$ may have on overall process efficiency as well as production costs was investigated. Since the compression of $H_2$ is energy-intensive, reducing the pressure ratio between the coupled processes could promote the effectiveness of the implemented $H_2$ loop. Under the assumption that the reaction system is not affected by the shift in pressure and the absorption behavior of formaldehyde in water is unchanged, $p_{SCP}$ was set at 5 bar for the following calculations. In these scenarios (110c-5, 200c-5 and 500c-5), feed dosing and subsequent heating of the SCP (see $P^1$, $P^2$, $C^5$, $C^6$, E, and $H^4$ in Fig. 2) have to be pressurized and the compression section for $CO_2$ and the $H_2$-rich recycle stream (see $C^1$ to $C^3$ in Fig. 2) at the inlet of methanol production is adapted accordingly. Calculated exergy efficiencies $\eta_{Ex,i}$ are given in Table 6.

It was found that with the reduced overall compression ratio between both subprocesses $\eta_{Ex,CH_3OH}$ is increased by 0.2%pt (500c-5) to 1.1%pt (110c-5) due to lowered electricity demand during feed compression and slightly decreased related investment costs. This exergy benefit is weakest for large production sites, because a large amount of additional $CO_2$ is required to reach the targeted methanol capacity. As any fresh $CO_2$ is assumed to be fed at atmospheric pressure, only a small fraction of feed gases is positively affected by the reduced pressure difference between both plants. Since compression of the inlet streams is now required for the SCP, $\eta_{Ex,CH_2O}$ is equally lowered by 0.7% pt in all scenarios. Total exergy efficiencies remain nearly unchanged when compared to the according unpressurized directly coupled scenarios (110c, 200c and 500c, Table 4).

Similar to process efficiency, plant economics are influenced by the adapted pressure level of the SCP (Table 7). *MSP* of methanol are lowered by 4 €·t$^{-1}$ (500c-5) to 27 €·t$^{-1}$ (110c-5) with the reduced compression ratio for $CO_2$ dosing. Again, the effect is largest for small plants, as only small amounts of fresh $CO_2$ are added to the feed stream. In contrast, formaldehyde becomes more expensive regardless of the lowered methanol price and its strong influence on *MSP* of formaldehyde (Fig. 8). With the addition of compressors for $CO_2$ and $O_2$ at the inlet of the SCP, capital investment for the subprocess is increased by a

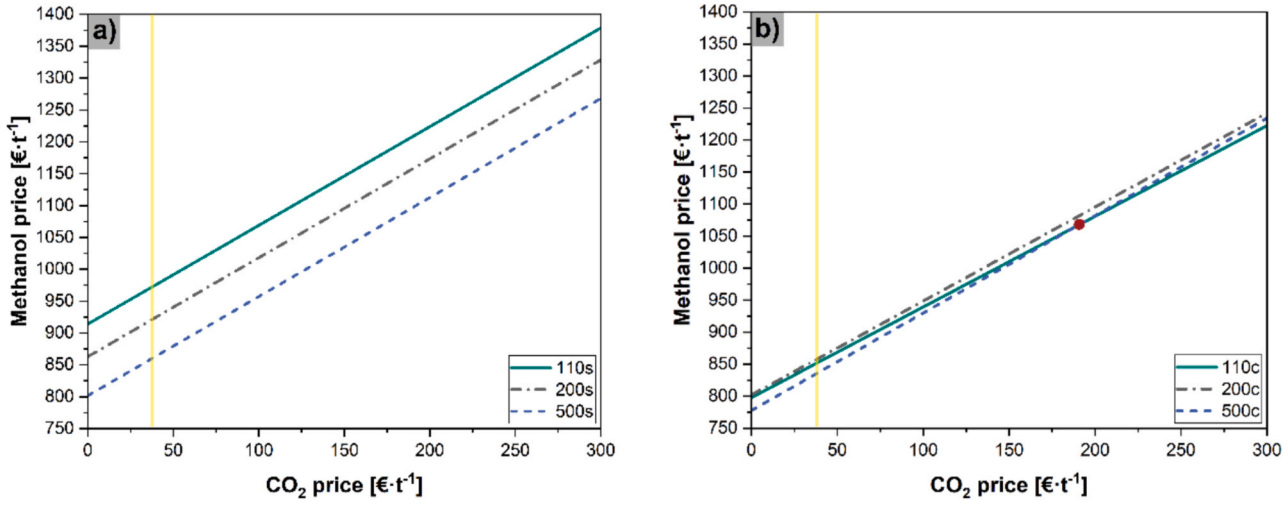


**Fig. 11.** *MSP* of methanol for separate (a)) and coupled (b)) process chains at different methanol capacities (110 kt·a$^{-1}$, 200 kt·a$^{-1}$ and 500 kt·a$^{-1}$) in dependence of $CO_2$ capture costs. Yellow lines mark initial values of the cost factor, red circles indicate a change in superiority of the regarded plant scales.

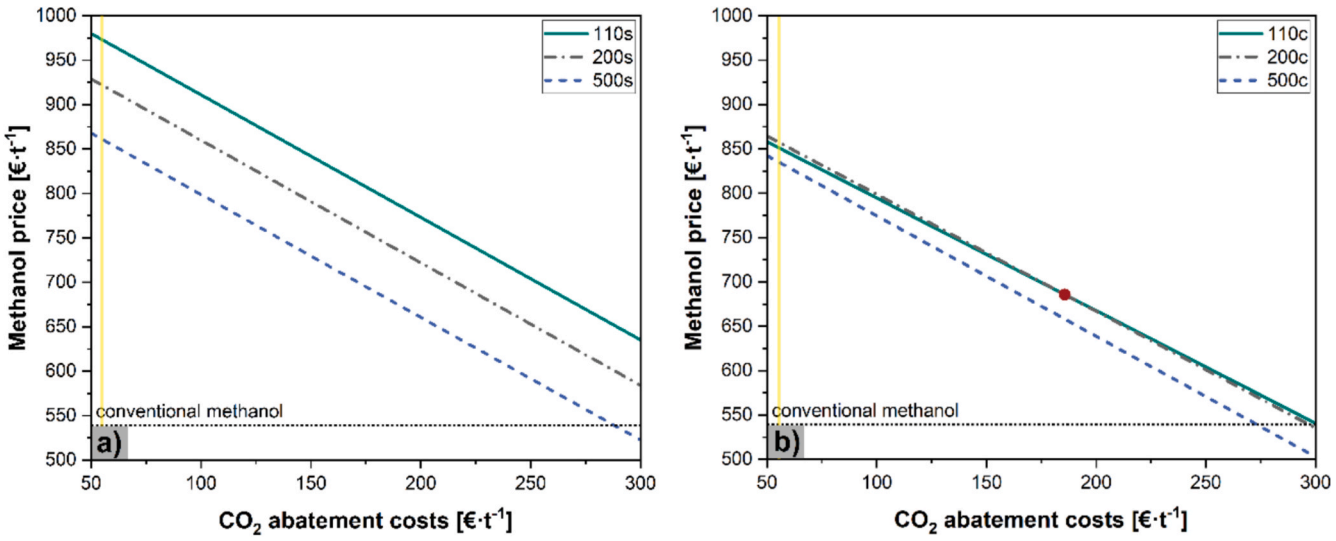


**Fig. 12.** Methanol price for separate (a)) and coupled (b)) process chains at different methanol capacities (110 kt·a$^{-1}$, 200 kt·a$^{-1}$ and 500 kt·a$^{-1}$) in relation to $CO_2$ abatement costs. The market price of conventional methanol (539 €·t$^{-1}$ in 2024) is given as reference [154]. Yellow lines mark initial values of the cost factor, red circles indicate a change in superiority of the regarded plant scales.

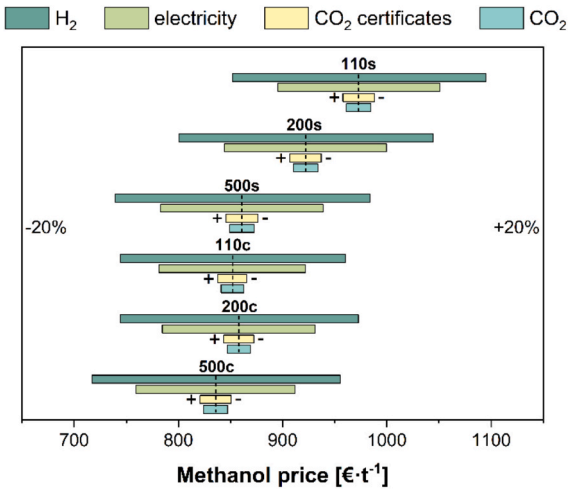


**Fig. 13.** Sensitivity of *MSP* of methanol regarding $H_2$, electricity, and $CO_2$ prices as well as costs of $CO_2$ certificates. Investigated parameters are varied ± 20% and nominal values of the presented techno-economic assessment are marked by dotted lines. Because the costs of $CO_2$ certificates are credited, they are plotted inversely.

**Table 6**
Exergy efficiencies calculated for the considered coupled (c) process chains with operating pressure of formaldehyde production $p_{SCP}$ set at 5 bar (5) at different methanol capacities (110 kt·a$^{-1}$, 200 kt·a$^{-1}$, 500 kt·a$^{-1}$). Differences to the corresponding base case are given in parentheses.

| Parameter | 110c-5 | 200c-5 | 500c-5 |
|---|---|---|---|
| $\eta_{E,CH_3OH}$ [%] | 89.5 (+1.1%pt) | 83.7 (+0.5%pt) | 80.2 (+0.2%pt) |
| $\eta_{E,CH_2O}$ [%] | 68.2 (−0.7%pt) | 68.4 (−0.7%pt) | 68.3 (−0.7%pt) |
| $\eta_{E,total}$ [%] | 61.0 (+0.1%pt) | 69.2 (±0%pt) | 74.6 (±0%pt) |

factor of 2.4. At the same time, more electricity is required to supply the raw materials to the process. Formaldehyde prices are between 43 €·t$^{-1}$ (110c-5) and 73 €·t$^{-1}$ (500c-5) higher than those of the unpressurized scenarios.

When considering total production capacity and the related annual production costs of both subprocesses, lowered selling prices for methanol cannot outweigh increased expenditures for the pressurized implementation of the SCP. Annual expenditures amount to 92.4 M€·a$^{-1}$ (110c-5), 162.7 M€·a$^{-1}$ (200c-5) and 385.8 M€·a$^{-1}$ (500c-5) if the operating pressure of the SCP is set at 5 bar. In comparison, only 88.7 M€·a$^{-1}$ (110c), 158.4 M€·a$^{-1}$ (200c) and 381.2 M€·a$^{-1}$ (500c) are spent, if the modified SCP is operated at atmospheric pressure. Reduced electricity demand and required capital investment for methanol production are countered by higher values of both quantities related to the SCP

**Table 7**
Calculated minimum selling prices (*MSP*) of methanol and formaldehyde for coupled (c) processes with operating pressure of formaldehyde production $p_{SCP}$ set at 5 bar (5) at different methanol capacities (110 kt·a$^{-1}$, 200 kt·a$^{-1}$ and 500 kt·a$^{-1}$).

| Product | *MSP* [€·t$^{-1}$] | | |
|---|---|---|---|
| | 110c-5 | 200c-5 | 500c-5 |
| Methanol | 825 (−27 €·t$^{-1}$) | 846 (−12 €·t$^{-1}$) | 832 (−4 €·t$^{-1}$) |
| Formaldehyde | 1166 (+43 €·t$^{-1}$) | 1193 (+62 €·t$^{-1}$) | 1179 (+74 €·t$^{-1}$) |

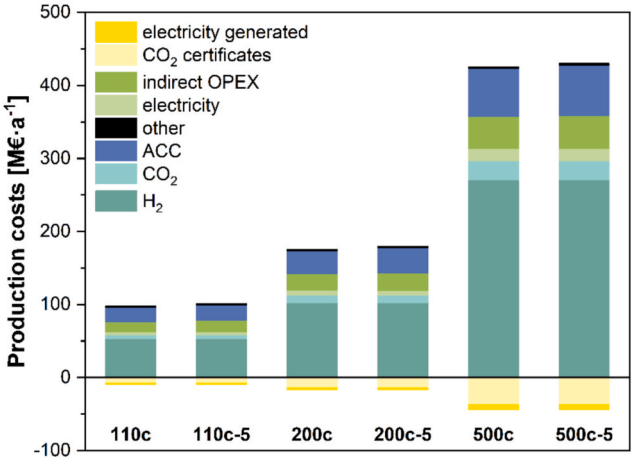


**Fig. 14.** Calculated overall annual production costs for directly coupled (c) methanol and formaldehyde production with operating pressure of formaldehyde production $p_{SCP}$ set at 5 bar (5) and at different methanol capacities (110 kt·a$^{-1}$, 200 kt·a$^{-1}$ and 500 kt·a$^{-1}$).

(Fig. 14). The same effects were also observed, if $p_{SCP}$ was raised only slightly to reach 3 bar or increased further to 10 bar. Ultimately, there is no enhanced energetic or economic advantage to be gained by increasing $p_{SCP}$ for the directly coupled production of methanol and formaldehyde.

## 5. Conclusion and outlook

As one of the limiting resources of the targeted carbon–neutral economy, sustainable $H_2$ has globally been in the spotlight of recent research. While many other sectors have already optimized $H_2$ utilization or are actively addressing the issue, the chemical industry still lags behind in this endeavor. With the expected increased charges for carbon-free $H_2$, the utilization of $H_2$-rich industrial waste streams may become a crucial instrument for the maximization of overall $H_2$ efficiency of chemical processes. To evaluate the potential of $H_2$ networks between otherwise independent processes, an exemplary case study was conducted. For this investigation, a $H_2$ loop was implemented between industrially scaled sites for $CO_2$-based methanol production and subsequent formaldehyde synthesis. The model case was chosen, because methanol is one of the most important building blocks of the chemical industry and its most relevant derivative, formaldehyde, is predominantly produced via the dehydrogenation of the alcohol. The resulting process pair includes one synthesis that applies $H_2$ as starting material while the other disposes of a $H_2$-rich byproduct by means of heat recovery.

As already established in previous work [105], an improvement in $H_2$ efficiency of up to 11%pt can be achieved by reusing the absorption off-gas of a modified SCP as partial feedstock for a preceding methanol synthesis. At the same time, $CO_2$ emissions of the overall process chain are reduced. Additionally, the presented study shows that supplied energy is used more efficiently in the suggested coupled production site. An enhancement of 1.2%pt to 4.5%pt was noted for the considered plant size range. Especially savings in fresh $H_2$ and the omission of intermediate methanol purification ultimately led to a reduction of minimum selling prices (*MSP*). With the mentioned advantages being proportionally larger for small plants, they become more lucrative than medium-scaled installations over a wide range of $H_2$ prices. As a result, decentralized plants with lower production capacities could particularly benefit from a joint network for $H_2$ exchange. In order to facilitate a quick rollout of a carbon–neutral economy, future process development should thus consider maximizing $H_2$ efficiency with the help of utilized $H_2$-rich byproducts and integrated $H_2$ loops.

Current work focuses on validating the feasibility of formaldehyde synthesis in the presence of large amounts of $CO_2$. Planned experimental studies include investigations on the influence of various operating parameters like partial pressure of $CO_2$, $H_2O$ and $O_2$, reaction temperature and gas hourly space velocities.

## CRediT authorship contribution statement

**Pia Münzer:** Writing – original draft, Methodology, Investigation, Formal analysis, Data curation, Conceptualization. **Bruno Lacerda de Oliveira Campos:** Writing – review & editing, Methodology. **Ulrich Arnold:** Writing – review & editing, Supervision, Project administration, Investigation. **Jörg Sauer:** Writing – review & editing, Supervision, Project administration, Methodology, Conceptualization.

## Declaration of competing interest

The authors declare that they have no known competing financial interests or personal relationships that could have appeared to influence the work reported in this paper.

## Appendix A. Supplementary data

Supplementary data to this article can be found online at https://doi.org/10.1016/j.enconman.2026.121216.

## Data availability

Data will be made available on request.

## References


[1] International Energy Agency. Global Hydrogen Review 2021:2021.
[2] International Energy Agency. Global Hydrogen Review 2024:2024.
[3] Jaunatre M. Renewable hydrogen: renewable energy and renewable hydrogen APAC markets policies analysis. Wiesbaden: Springer Fachmedien Wiesbaden GmbH; 2021.
[4] "Wasserstoff: Produktionskosten nach Typ bis 2050," available at https://de.statista.com/statistik/daten/studie/1195863/umfrage/produktionskosten-von-wasserstoff-nach-wasserstofftyp-in-deutschland/, 2025.
[5] Zimmermann H, Walzl R. in Ullmann's Encyclopedia of Industrial Chemistry (Ed: Wiley-VCH Verlag GmbH & Co. KGaA): Wiley-VCH Verlag GmbH & Co. KGaA, Weinheim, Germany; 2009.
[6] Zimmermann H. Ullmann's Encyclopedia of Industrial Chemistry (Ed: Wiley-VCH). 1st ed. Wiley; 2013.
[7] O'Brien T, Bommaraju TV, Hine F. Handbook of Chlor-Alkali Technology. New York: Springer; 2005.
[8] D.-Y. Lee, A. A. Elgowainy, Q. Dai, Life Cycle Greenhouse Gas Emissions of By-Product Hydrogen from Chlor-Alkali Plants 2017.
[9] Chlor-Alkali Industry Review 2023-2024, Eurochlor 2024.
[10] A. W. Franz, H. Kronemayer, D. Pfeiffer, R. D. Pilz, G. Reuss, W. Disteldorf, A. O. Gamer, A. Hilt, in Ullmann's Encyclopedia of Industrial Chemistry (Ed: Wiley-VCH Verlag GmbH & Co. KGaA), Wiley-VCH Verlag GmbH & Co. KGaA, Weinheim, Germany 2016.
[11] Sperber H. Chem Ing Tech 1969;41(17):962–6. https://doi.org/10.1002/cite.330411705.
[12] Millar GJ, Collins M. Ind Eng Chem Res 2017;56(33):9247–65. https://doi.org/10.1021/acs.iecr.7b02388.
[13] M. Bertau, Methanol: The Basic Chemical and Energy Feedstock of the Future Asinger's Vision Today Based on "Methanol - Chemie- Und Energierohstoff: Die Mobilisation Der Kohle" by Friedrich Asinger Published in 1986 Includes Contributions by More than 40 Experts from Industry and Academia, Springer, Berlin [u.a.] 2014.
[14] B. Lacerda De Oliveira Campos, K. Herrera Delgado, S. Wild, F. Studt, S. Pitter, J. Sauer, React. Chem. Eng. 2021, 6 (5), 868–887. DOI: 10.1039/D1RE00040C.
[15] Olah GA, Goeppert A, Prakash GKS. J Org Chem 2009;74(2):487–98. https://doi.org/10.1021/jo801260f.
[16] Xie S, Zhang W, Lan X, Lin H. ChemSusChem 2020;13(23):6141–59. https://doi.org/10.1002/cssc.202002087.
[17] Guil-López R, Mota N, Llorente J, Millán E, Pawelec B, Fierro JLG, et al. Materials 2019;12(23):3902. https://doi.org/10.3390/ma12233902.
[18] Stangeland K, Li H, Yu Z. Ind Eng Chem Res 2018;57(11):4081–94. https://doi.org/10.1021/acs.iecr.7b04866.
[19] Bos MJ, Slotboom Y, Kersten SRA, Brilman DWF. Ind Eng Chem Res 2019;58(31):13987–99. https://doi.org/10.1021/acs.iecr.9b02576.
[20] Li H, Wang L, Xiao F-S. Catal Today 2023;418:114051. https://doi.org/10.1016/j.cattod.2023.114051.
[21] Zhang H, Chen J, Han X, Pan Y, Hao Z, Tang S, et al. Ind Eng Chem Res 2024;63(14):6210–21. https://doi.org/10.1021/acs.iecr.4c00357.
[22] HIF, "HIF Global," available at https://hifglobal.com/, 2025.
[23] Carbon Recycling International, "Global Leader in CO2 to Methanol Technology," available at https://carbonrecycling.com, 2025.
[24] "Methanol: Globale Produktionskapazität bis 2023," available at https://de.statista.com/statistik/daten/studie/1454582/umfrage/methanol-globale-produktionskapazitaet/, n.d.
[25] Ott J, Gronemann V, Pontzen F, Fiedler E, Grossmann G, Kersebohm DB, et al. Ullmann's Encyclopedia of Industrial Chemistry (Ed: Wiley-VCH). 1st ed. Wiley; 2012.
[26] Tabibian SS, Sharifzadeh M. Renew Sustain Energy Rev 2023;179:113281. https://doi.org/10.1016/j.rser.2023.113281.
[27] Baerns M, Behr A, Brehm A, Gmehling J, Hinrichsen K-O, Hofmann H, et al. Technische Chemie, Dritte. Auflage ed. Weinheim: Ernst & Sohn; 2023.
[28] "Chlorine global market volume 2030," available at https://www.statista.com/statistics/1310477/chlorine-market-volume-worldwide/, n.d.
[29] Commission of the European Union. Joint Research Centre. Institute for Prospective Technological Studies., Best Available Techniques (BAT) Reference Document for Iron and Steel Production: Industrial Emissions Directive 2010/75/EU : Integrated Pollution Prevention and Control., Publications Office, LU 2013.
[30] Frey A, Goeke V, Voss C. Chem Ing Tech 2018;90(10):1384–91. https://doi.org/10.1002/cite.201800046.
[31] Liao H, Li B, Zhang B. Fuel 1998;77(14):1643–6. https://doi.org/10.1016/S0016-2361(98)00076-3.
[32] Lafyatis DS, Creten G, Froment GF. Appl Catal A 1994;120(1):85–103. https://doi.org/10.1016/0926-860X(94)80335-8.

[33] J. Sauer, M. Bewersdorf, M. Köstner, M. Rinner, D. Wolf, Hydrocyanic Acid (HCN) Production, 2nd, completely revised and enlarged ed ed., Vol. 5, Wiley-VCH, Weinheim 2008.
[34] Endter F. Chem Ing Tech 1958;30(5):305–10. https://doi.org/10.1002/cite.330300506.
[35] Andrussow L. Angew Chem 1935;48(37):593–5. https://doi.org/10.1002/ange.19350483702.
[36] Andrussow L. Angew Chem 1951;63(1):21–7. https://doi.org/10.1002/ange.19510630106.
[37] Nnabuife SG, Ugbeh-Johnson J, Okeke NE, Ogbonnaya C. Carbon Capture Sci Technol 2022;3:100042. https://doi.org/10.1016/j.ccst.2022.100042.
[38] Van Der Spek M, Banet C, Bauer C, Gabrielli P, Goldthorpe W, Mazzotti M, et al. Energy Environ Sci 2022;15(3):1034–77. https://doi.org/10.1039/D1EE02118D.
[39] Hui Y, Wang M, Guo S, Akhtar S, Bhattacharya S, Dai B, et al. Energ Conver Manage 2024;315:118776. https://doi.org/10.1016/j.enconman.2024.118776.
[40] Wang C, Li Y, Wan J, Hu Y. Int J Hydrogen Energy 2024;67:942–8. https://doi.org/10.1016/j.ijhydene.2024.02.138.
[41] Zhang X, Qian X, Xiao C, Yin X, Wang X, Wang Z, et al. Green Energy Resour 2024;2(4):100098. https://doi.org/10.1016/j.gerr.2024.100098.
[42] Guo L, Wu Z, Wang H, Yan H, Yang F, Cheng G, et al. Chem Eng J 2023;455:140689. https://doi.org/10.1016/j.cej.2022.140689.
[43] Towler GP, Mann R, Serriere A-L, Gebaude CMD. Ind Eng Chem Res 1996;35:2378–88.
[44] Alves JJ, Towler GP. Ind Eng Chem Res 2002;41(23):5759–69. https://doi.org/10.1021/ie010558v.
[45] Liu X, Liu J, Deng C, Lee J-Y, Tan RR. Energy 2020;201:117623. https://doi.org/10.1016/j.energy.2020.117623.
[46] Gai L, Varbanov PS, Fan YV, Klemeš JJ, Nižetić S. Int J Hydrogen Energy 2022;47(24):12159–78. https://doi.org/10.1016/j.ijhydene.2021.06.154.
[47] Shen Y, Lou Y, Ren C, Hong X, Liao Z, Wang J, et al. Int J Hydrogen Energy 2022;47(2):848–61. https://doi.org/10.1016/j.ijhydene.2021.10.071.
[48] Deng C, Zhou Y, Jiang W, Feng X. Int J Hydrogen Energy 2017;42(31):19984–20002. https://doi.org/10.1016/j.ijhydene.2017.06.199.
[49] Kang L, Liang X, Liu Y. Int J Hydrogen Energy 2018;43(34):16638–51. https://doi.org/10.1016/j.ijhydene.2018.07.044.
[50] Lou Y, Liao Z, Sun J, Jiang B, Wang J, Yang Y. Int J Hydrogen Energy 2019;44(12):5686–95. https://doi.org/10.1016/j.ijhydene.2019.01.099.
[51] Shehata WM. Egypt J Pet 2016;25(4):539–53. https://doi.org/10.1016/j.ejpe.2015.12.002.
[52] Shehata WM, Shoaib AM, Gad FK. Egypt J Pet 2018;27(4):553–65. https://doi.org/10.1016/j.ejpe.2017.08.006.
[53] Moral G, Ortiz-Imedio R, Ortiz A, Gorri D, Ortiz I. Ind Eng Chem Res 2022;61(18):6106–24. https://doi.org/10.1021/acs.iecr.1c04668.
[54] Guo R, Li L, Chang C, Di Z. J Clean Prod 2022;379:134778. https://doi.org/10.1016/j.jclepro.2022.134778.
[55] Razzaq R, Li C, Zhang S. Fuel 2013;113:287–99. https://doi.org/10.1016/j.fuel.2013.05.070.
[56] Bermúdez JM, Arenillas A, Luque R, Menéndez JA. Fuel Process Technol 2013;110:150–9. https://doi.org/10.1016/j.fuproc.2012.12.007.
[57] Liu W, Zuo H, Wang J, Xue Q, Ren B, Yang F. Int J Hydrogen Energy 2021;46(17):10548–69. https://doi.org/10.1016/j.ijhydene.2020.12.123.
[58] Lee B, Kim H, Lee H, Byun M, Won W, Lim H. Renew Sustain Energy Rev 2020;133:110056. https://doi.org/10.1016/j.rser.2020.110056.
[59] Liu H, Guo W. Fuel 2023;332:125706. https://doi.org/10.1016/j.fuel.2022.125706.
[60] Wang B, Shao Y, Guo K, Li X, Yang L, Sun M, et al. Energ Conver Manage 2025;332:119777. https://doi.org/10.1016/j.enconman.2025.119777.
[61] Yi Q, Gong M-H, Huang Y, Feng J, Hao Y-H, Zhang J-L, et al. Energy 2016;112:618–28. https://doi.org/10.1016/j.energy.2016.06.111.
[62] Xiang D, Xiang J, Sun Z, Cao Y. Energy 2017;140:78–91. https://doi.org/10.1016/j.energy.2017.08.058.
[63] Gao R, Zhang C, Kwak G, Lee Y-J, Kang SC, Guan G. Energ Conver Manage 2020;213:112819. https://doi.org/10.1016/j.enconman.2020.112819.
[64] Gong M, Yi Q, Huang Y, Wu G, Hao Y, Feng J, et al. Energ Conver Manage 2017;133:318–31. https://doi.org/10.1016/j.enconman.2016.12.010.
[65] Kim S, Kim J. Fuel 2020;266:117093. https://doi.org/10.1016/j.fuel.2020.117093.
[66] Shin S, Lee J-K, Lee I-B. Energy 2020;200:117506. https://doi.org/10.1016/j.energy.2020.117506.
[67] Xu Y-P, Liu R-H, Shen M-Z, Lv Z-A, Chupradit S, Metwally ASM, et al. Sustainable Prod Consumption 2022;32:318–29. https://doi.org/10.1016/j.spc.2022.05.005.
[68] Zhao Y, Zhao Y, Yi Q, Li T, Wang J, Bao W, et al. Energ Conver Manage 2021;248:114796. https://doi.org/10.1016/j.enconman.2021.114796.
[69] Zhao Y, Zhao Y, Wang J, Bao W, Chang L. Int J Hydrogen Energy 2023;48(99):39330–46. https://doi.org/10.1016/j.ijhydene.2023.08.055.
[70] Kim S, Kim M, Kim YT, Kwak G, Kim J. Energ Conver Manage 2019;182:240–50. https://doi.org/10.1016/j.enconman.2018.12.037.
[71] Park H, Woo Y, Jung HS, Kim G, Bae JW, Park M-J. J Clean Prod 2021;326:129367. https://doi.org/10.1016/j.jclepro.2021.129367.
[72] Hauser A, Weitzer M, Gunsch S, Neubert M, Karl J. Fuel Process Technol 2021;217:106701. https://doi.org/10.1016/j.fuproc.2020.106701.
[73] Frosch RA, Gallopoulos NE. Sci Am 1989;261(3):144–53.
[74] Côté R, Hall J. J Clean Prod 1995;3(1–2):41–6. https://doi.org/10.1016/0959-6526(95)00041-C.
[75] Lowe EA. J Clean Prod 1997;5(1–2):57–65. https://doi.org/10.1016/S0959-6526(97)00017-6.
[76] Boix M, Montastruc L, Azzaro-Pantel C, Domenech S. J Clean Prod 2015;87:303–17. https://doi.org/10.1016/j.jclepro.2014.09.032.
[77] Butturi MA, Lolli F, Sellitto MA, Balugani E, Gamberini R, Rimini B. Appl Energy 2019;255:113825. https://doi.org/10.1016/j.apenergy.2019.113825.
[78] Ehrenfeld J, Gertler N. J Indus Ecol 1997;1(1):67–79. https://doi.org/10.1162/jiec.1997.1.1.67.
[79] Heeres RR, Vermeulen WJV, De Walle FB. J Clean Prod 2004;12(8–10):985–95. https://doi.org/10.1016/j.jclepro.2004.02.014.
[80] Chertow M, Ehrenfeld J. J Indus Ecol 2012;16(1):13–27. https://doi.org/10.1111/j.1530-9290.2011.00450.x.
[81] Yu F, Han F, Cui Z. J Clean Prod 2015;87:339–47. https://doi.org/10.1016/j.jclepro.2014.10.058.
[82] Affery AP, Tan JX, Ong IYB, Lim JY, Yoo C, How BS, et al. Process Saf Environ Prot 2021;155:197–218. https://doi.org/10.1016/j.psep.2021.08.016.
[83] Kantor I, Fowler M, Elkamel A. Int J Hydrogen Energy 2012;37(6):5347–59. https://doi.org/10.1016/j.ijhydene.2011.08.084.
[84] Thun SQ, Chew IML. J Clean Prod 2024;476:143736. https://doi.org/10.1016/j.jclepro.2024.143736.
[85] Kuznetsov M, Boldyryev S, Kenzhebekov D, Kaldybaeva B. Int J Hydrogen Energy 2022;47(74):31755–72. https://doi.org/10.1016/j.ijhydene.2021.12.184.
[86] Fawwaz A, Nugraha APA, Al Rasyid MP, Muhammad RH. J Chem Eng Res Prog 2025;2(1):115–21. https://doi.org/10.9767/jcerp.20301.
[87] Xiang D, Li P, Xia Y. Energ Conver Manage 2023;281:116820. https://doi.org/10.1016/j.enconman.2023.116820.
[88] Lacerda De Oliveira Campos B, John K, Beeskow P, Herrera Delgado K, Pitter S, Dahmen N, Sauer J. Processes 2022;10(8):1535. https://doi.org/10.3390/pr10081535.
[89] Cordero-Lanzac T, Ramirez A, Navajas A, Gevers L, Brunialti S, Gandía LM, et al. J Energy Chem 2022;68:255–66. https://doi.org/10.1016/j.jechem.2021.09.045.
[90] Anicic B, Trop P, Goricanec D. Energy 2014;77:279–89. https://doi.org/10.1016/j.energy.2014.09.069.
[91] Kourkoumpas DS, Papadimou E, Atsonios K, Karellas S, Grammelis P, Kakaras E. Int J Hydrogen Energy 2016;41(38):16674–87. https://doi.org/10.1016/j.ijhydene.2016.07.100.
[92] Battaglia P, Buffo G, Ferrero D, Santarelli M, Lanzini A. J CO2 Util 2021;44:101407. https://doi.org/10.1016/j.jcou.2020.101407.
[93] De Fournas N, Wei M. Energ Conver Manage 2022;257:115440. https://doi.org/10.1016/j.enconman.2022.115440.
[94] Schorn F, Breuer JL, Samsun RC, Schnorbus T, Heuser B, Peters R, et al. Adv Appl Energy 2021;3:100050. https://doi.org/10.1016/j.adapen.2021.100050.
[95] Zang G, Sun P, Elgowainy A, Wang M. Environ Sci Technol 2021;55(8):5248–57. https://doi.org/10.1021/acs.est.0c08237.
[96] Szima S, Cormos C-C. J CO2 Util 2018;24:555–63. https://doi.org/10.1016/j.jcou.2018.02.007.
[97] Nguyen TBH, Zondervan E. J CO2 Util 2019;34:1–11. https://doi.org/10.1016/j.jcou.2019.05.033.
[98] Alsayegh S, Johnson JR, Ohs B, Wessling M. J Clean Prod 2019;208:1446–58. https://doi.org/10.1016/j.jclepro.2018.10.132.
[99] Adnan MA, Kibria MG. Appl Energy 2020;278:115614. https://doi.org/10.1016/j.apenergy.2020.115614.
[100] Sollai S, Porcu A, Tola V, Ferrara F, Pettinau A. J CO2 Util 2023;68:102345. https://doi.org/10.1016/j.jcou.2022.102345.
[101] Harris K, Grim RG, Huang Z, Tao L. Appl Energy 2021;303:117637. https://doi.org/10.1016/j.apenergy.2021.117637.
[102] Gu Y, Wang D, Chen Q, Tang Z. Int J Hydrogen Energy 2022;47(8):5085–100. https://doi.org/10.1016/j.ijhydene.2021.11.148.
[103] Charoensuppanimit P, Kitsahawong K, Kim-Lohsoontorn P, Assabumrungrat S. J Clean Prod 2019;212:893–909. https://doi.org/10.1016/j.jclepro.2018.12.010.
[104] Mantei F, Ali RE, Baensch C, Voelker S, Haltenort P, Burger J, et al. Sustainable Energy Fuels 2022;6(3):528–49. https://doi.org/10.1039/D1SE01270C.
[105] Münzer P, Arnold U, Sauer J. Chem Ing Tech 2024;96(6):819–25. https://doi.org/10.1002/cite.202300183.
[106] Towler GP, Sinnott RK. Chemical Engineering Design: Principles, Practice, and Economics of Plant and Process Design. 2nd ed. Boston, MA: Butterworth-Heinemann; 2013.
[107] Bozzano G, Manenti F. Prog Energy Combust Sci 2016;56:71–105. https://doi.org/10.1016/j.pecs.2016.06.001.
[108] Bussche KMV, Froment GF. J Catal 1996;161(1):1–10. https://doi.org/10.1006/jcat.1996.0156.
[109] Wu J, Saito M, Takeuchi M, Watanabe T. Appl Catal A 2001;218(1–2):235–40. https://doi.org/10.1016/S0926-860X(01)00650-0.
[110] Prašnikar A, Pavlišič A, Ruiz-Zepeda F, Kovač J, Likozar B. Ind Eng Chem Res 2019;58(29):13021–9. https://doi.org/10.1021/acs.iecr.9b01898.
[111] L. Pilato, Ed., Phenolic Resins: A Century of Progress, Springer, Heidelberg : New York 2010.
[112] Masamoto J, Matsuzaki K, Morishita H. J Appl Polym Sci 1993;50(8):1307–15. https://doi.org/10.1002/app.1993.070500802.
[113] Liu H, Gao H, Ma Y, Gao Z, Eli W. Chem Eng Technol 2012;35(5):841–6. https://doi.org/10.1002/ceat.201100446.
[114] McGill PR, Söhnel T. PCCP 2012;14(2):858–68. https://doi.org/10.1039/C1CP22887K.
[115] Sun J, Li H, Song H, Wu Q, Zhao Y, Jiao Q. RSC Adv 2015;5(106):87200–5. https://doi.org/10.1039/C5RA18598J.
[116] Ahn S, You Y-W, Lee D-G, Kim K-H, Oh M, Lee C-H. Chem Eng Sci 2012;68(1):413–23. https://doi.org/10.1016/j.ces.2011.09.053.

[117] Banu A-M, Friedrich D, Brandani S, Düren T. Ind Eng Chem Res 2013;52(29):9946–57. https://doi.org/10.1021/ie4011035.
[118] Yang J, Lee C. AIChE J 1998;44(6):1325–34. https://doi.org/10.1002/aic.690440610.
[119] A. Aicher, H. Haas, H. Diem, C. Dudeck, F. Brunnmüller, G. Lehmann, Manufacture of Concentrated Aqueous Solutions of Formaldehyde, US4119673A, n.d.
[120] Walker JF. Formaldehyde. 3rd ed. Reinhold Publishing Corporation; 1944.
[121] Winnacker K, Küchler L, Dittmeyer R, editors. Chemische Technik: Prozesse und Produkte, 5. Aufl. ed. Weinheim: Wiley-VCH; 2004.
[122] Wiesmann T, Hamel C, Kaluza S. Chem Ing Tech 2018;90(10):1446–52. https://doi.org/10.1002/cite.201800022.
[123] Van-Dal ÉS, Bouallou C. J Clean Prod 2013;57:38–45. https://doi.org/10.1016/j.jclepro.2013.06.008.
[124] Kiss AA, Pragt; JJ, Vos HJ, Bargeman G, De Groot MT. Chem Eng J 2016;284:260–9. https://doi.org/10.1016/j.cej.2015.08.101.
[125] Nieminen H, Laari A, Koiranen T. Processes 2019;7(7):405. https://doi.org/10.3390/pr7070405.
[126] Lacerda De Oliveira Campos B, Herrera Delgado K, Pitter S, Sauer J. Ind Eng Chem Res 2021;60(42):15074–86. https://doi.org/10.1021/acs.iecr.1c02952.
[127] Waterhouse GIN, Bowmaker GA, Metson JB. Appl Catal A 2004;265(1):85–101. https://doi.org/10.1016/j.apcata.2004.01.016.
[128] Lefferts L, Van Ommen JG, Ross JRH. Appl Catal 1986;23(2):385–402. https://doi.org/10.1016/S0166-9834(00)81306-8.
[129] Andreasen A, Lynggaard H, Stegelmann C, Stoltze P. Surf Sci 2003;544(1):5–23. https://doi.org/10.1016/j.susc.2003.08.007.
[130] Wachs IE, Madix RJ. Surf Sci 1978;76(2):531–58. https://doi.org/10.1016/0039-6028(78)90113-9.
[131] Vanveen A, Hinrichsen O, Muhler M. J Catal 2002;210(1):53–66. https://doi.org/10.1006/jcat.2002.3682.
[132] G. Halbritter, W. Mühlthaler, H. Sperber, H. Diem, C. Dudeck, G. Lehmann, Manufacture of Formaldehyde, US4072717A, n.d.
[133] A. Aicher, H. Haas, H. Sperber, H. Diem, G. Matthias, G. Lehmann, Production of Formaldehyde, US4010208A, n.d.
[134] D. Wolf, H. Diem, O. Grabowsky, G. Matthias, Manufacture of Formaldehyde, US4209466A, n.d.
[135] Bongartz D, Burre J, Mitsos A. Ind Eng Chem Res 2019;58(12):4881–9. https://doi.org/10.1021/acs.iecr.8b05576.
[136] Mignard D, Pritchard C. Chem Eng Res Des 2006;84(9):828–36. https://doi.org/10.1205/cherd.05204.
[137] Strauß K. Kraftwerkstechnik: zur Nutzung fossiler, nuklearer und regenerativer Energiequellen. 7. Aufl 2016 ed.,. Berlin Heidelberg, Berlin, Heidelberg: Springer; 2016.
[138] Crouch H, Carver EK. Ind Eng Chem 1925;7(6):641–2.
[139] Molnarne M, Mizsey P, Schroder V. J Hazard Mater 2005;121(1–3):45–9. https://doi.org/10.1016/j.jhazmat.2005.01.033.
[140] Di Benedetto A, Di Sarli V, Salzano E, Cammarota F, Russo G. Int J Hydrogen Energy 2009;34(16):6970–8. https://doi.org/10.1016/j.ijhydene.2009.05.120.
[141] Grune J, Breitung W, Kuznetsov M, Yanez J, Jang W, Shim W. Int J Hydrogen Energy 2015;40(31):9838–46. https://doi.org/10.1016/j.ijhydene.2015.06.004.
[142] Wang ZR, Ni L, Liu X, Jiang JC, Wang R. J Loss Prev Process Ind 2014;31:10–5. https://doi.org/10.1016/j.jlp.2014.06.004.
[143] Kumar R, Huggahalli M, Deng S, Andrecovich M. Adsorption 2003;9(3):243–50. https://doi.org/10.1023/A:1024701917647.
[144] Razak AA, Saaid IM, Yusof MAM, Husein N, Zaidin MF, Mohamad Sabil K. J Petrol Explor Prod Technol 2023;13(5):1235–46. https://doi.org/10.1007/s13202-023-01616-3.
[145] Albrecht FG, König DH, Baucks N, Dietrich R-U. Fuel 2017;194:511–26. https://doi.org/10.1016/j.fuel.2016.12.003.
[146] M. S. Peters, K. D. Timmerhaus, R. E. West, R. E. West, Plant Design and Economics for Chemical Engineers, 5. ed., international ed ed., McGraw-Hill, Boston 2003.
[147] R. Turton, Ed., Analysis, Synthesis, and Design of Chemical Processes, 4th ed ed., Prentice Hall, Upper Saddle River, NJ 2012.
[148] von Weizsäcker CC. Interdisziplinäre Aspekte der Energiewirtschaft. Wiesbaden: Springer Fachmedien Wiesbaden GmbH; 2016.
[149] Budinis S, Krevor S, Dowell NM, Brandon N, Hawkes A. Energ Strat Rev 2018;22:61–81. https://doi.org/10.1016/j.esr.2018.08.003.
[150] Fasihi M, Efimova O, Breyer C. J Clean Prod 2019;224:957–80. https://doi.org/10.1016/j.jclepro.2019.03.086.
[151] Zhang C, Conf IOP. Ser.: Earth Environ Sci 2021;657(1):012045. https://doi.org/10.1088/1755-1315/657/1/012045.
[152] Mofarahi M, Khojasteh Y, Khaledi H, Farahnak A. Energy 2008;33(8):1311–9. https://doi.org/10.1016/j.energy.2008.02.013.
[153] "CO2-Preis für Kohle- und Abfallbrennstoffe | Bundesregierung," available at https://www.bundesregierung.de/breg-de/aktuelles/co2-preis-kohle-abfallbrennstoffe-2061622, 2025.
[154] "Methanol: Preise auf dem europäischen Markt bis 2025," available at https://de.statista.com/statistik/daten/studie/730823/umfrage/durchschnittlicher-preis-fuer-methanol-auf-dem-europaeischen-markt/, 2025.
[155] E. C. D. Tan, M. Talmadge, A. Dutta, J. Hensley, J. Schaidle, M. J. Biddy, Process Design and Economics for the Conversion of Lignocellulosic Biomass to Hydrocarbons via Indirect Liquefaction 2015.
[156] S. D. Phillips, J. K. Tarud, M. J. Biddy, A. Dutta, Gasoline from Wood via Integrated Gasification, Synthesis, and Methanol-to-Gasoline Technologies 2011.
[157] Adler B. Strategische Metalle - Eigenschaften. Springer Spektrum, Berlin Heidelberg: Anwendung und Recycling; 2017.
[158] "Gehaltsvergleich," available at https://www.destatis.de/DE/Service/Statistik-Visualisiert/Gehaltsvergleich/_inhalt.html, 2025.
[159] Huang Y, Zhu L, He Y, Wang Y, Hao Q, Zhu Y. Energy 2023;273:127219. https://doi.org/10.1016/j.energy.2023.127219.
[160] Rihko-Struckmann LK, Peschel A, Hanke-Rauschenbach R, Sundmacher K. Ind Eng Chem Res 2010;49(21):11073–8. https://doi.org/10.1021/ie100508w.
[161] Methanex. 2025. available at https://www.methanex.com/about-methanol/pricing/.
[162] Jensen SH, Larsen PH, Mogensen M. Int J Hydrogen Energy 2007;32(15):3253–7. https://doi.org/10.1016/j.ijhydene.2007.04.042.
[163] Jang D, Kim J, Kim D, Han W-B, Kang S. Energ Conver Manage 2022;258:115499. https://doi.org/10.1016/j.enconman.2022.115499.
[164] Vartiainen E, Breyer C, Moser D, Román Medina E, Busto C, Masson G, et al. Sol RRL 2022;6(5):2100487. https://doi.org/10.1002/solr.202100487.
[165] Dubey A, Arora A. J Clean Prod 2022;373:133932. https://doi.org/10.1016/j.jclepro.2022.133932.
[166] Garcia JA, Villen-Guzman M, Rodriguez-Maroto JM, Paz-Garcia JM. J Environ Chem Eng 2022;10(5):108470. https://doi.org/10.1016/j.jece.2022.108470.
[167] Chauvy R, Dubois L. Intl J Energy Res 2022;46(8):10320–44. https://doi.org/10.1002/er.7884.
[168] Pires JCM, Martins FG, Alvim-Ferraz MCM, Simões M. Chem Eng Res Des 2011;89(9):1446–60. https://doi.org/10.1016/j.cherd.2011.01.028.
[169] Yun S, Oh S-Y, Kim J-K. Appl Energy 2020;268:114933. https://doi.org/10.1016/j.apenergy.2020.114933.